J Physiol Sci (2009) 59:3–21
DOI 10.1007/s12576-008-0008-4

REVIEW

The maxi-anion channel: a classical channel playing novel roles through an unidentified molecular entity

Ravshan Z. Sabirov · Yasunobu Okada

Received: 24 September 2008 / Accepted: 5 November 2008 / Published online: 9 December 2008

Abstract The maxi-anion channel is widely expressed and found in almost every part of the body. The channel is activated in response to osmotic cell swelling, to excision of the membrane patch, and also to some other physiologically and pathophysiologically relevant stimuli, such as salt stress in kidney macula densa as well as ischemia/hypoxia in heart and brain. Biophysically, the maxi-anion channel is characterized by a large single-channel conductance of 300–400 pS, which saturates at 580–640 pS with increasing the Cl^- concentration. The channel discriminates well between Na^+ and Cl^-, but is poorly selective to other halides exhibiting weak electric-field selectivity with an Eisenman's selectivity sequence I. The maxi-anion channel has a wide pore with an effective radius of $\sim$1.3 nm and permits passage not only of Cl^- but also of some intracellular large organic anions, thereby releasing major extracellular signals and gliotransmitters such as glutamate$^-$ and ATP^{4-}. The channel-mediated efflux of these signaling molecules is associated with kidney tubuloglomerular feedback, cardiac ischemia/hypoxia, as well as brain ischemia/hypoxia and excitotoxic neurodegeneration. Despite the ubiquitous expression, well-defined properties and physiological/pathophysiological significance of this classical channel, the molecular entity has not been identified. Molecular identification of the maxi-anion channel is an urgent task that would greatly promote investigation in the fields not only of anion channel but also of physiological/pathophysiological signaling in the brain, heart and kidney.

Keywords Maxi-anion channel · Volume-sensitive chloride channel · Purinergic signaling · ATP release · Glutamate release

R. Z. Sabirov · Y. Okada (✉)
Department of Cell Physiology,
National Institute for Physiological Sciences,
Okazaki 444-8585, Japan
e-mail: okada@nips.ac.jp

R. Z. Sabirov
Laboratory of Molecular Physiology,
Institute of Physiology and Biophysics,
Tashkent 100095, Uzbekistan

Y. Okada
Department of Physiological Sciences, School of Life Science,
The Graduate University for Advanced Studies (Sokendai),
Okazaki 444-8585, Japan

Introduction

Osmotic cell swelling induces activation of a large anionic conductance with characteristic outward rectification and voltage-dependent inactivation at high positive potentials. When the swelling-activated anion channels were studied at the single channel level, different types of event were described. In most cases, the event of volume-sensitive outwardly rectifying anion channel (VSOR) with an intermediate conductance of 30–70 pS has been described [1]. Consistent with the phenotype of the whole-cell VSOR current, this channel current exhibits outward rectification and voltage-dependent inactivation at large positive potentials (>+50 to +100 mV). However, many authors have also reported the single-channel event with a much larger unitary conductance (300–400 pS) observed in the cell-attached mode after cell swelling [2–9]. A representative example of the maxi-anion channel currents recorded in the cell-attached patch on an osmotically swollen mammary C127 cells is shown in Fig. 1a, b (open circles). Also, the maxi-anion channel

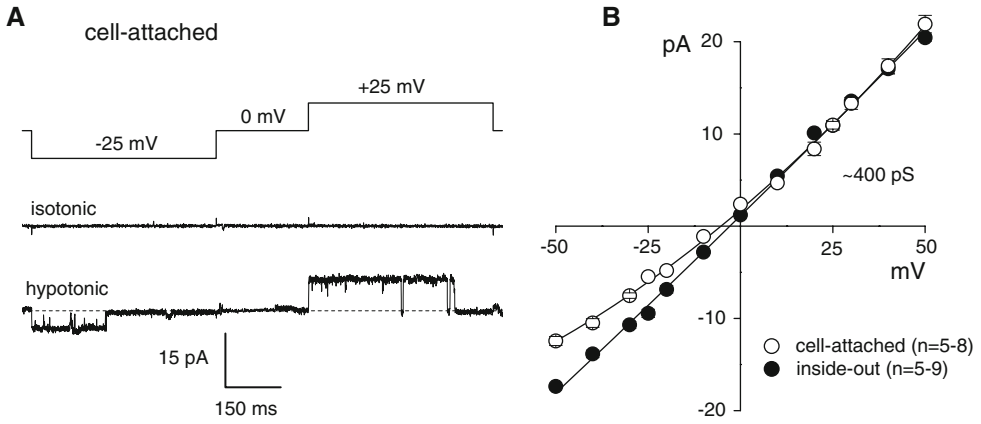

Fig. 1 Single-channel recordings of maxi-anion channel currents in on-cell patches activated by osmotic swelling of mammary C127 cells and in inside-out patches excised from the cells. **a** Representative current traces recorded under isotonic and hypotonic conditions on C127 cells during application of alternating pulses from 0 to ±25 mV (protocol is shown at the top of the traces). **b** Unitary I–V relationships for the single-channel events recorded in on-cell patches (*open circles*) and in inside-out patches (*filled circles*). Each symbol represents the mean ± SEM (*vertical bar*). Modified from Sabirov et al. [8]

is activated by excision of the inside-out patch (Fig. 1b, filled circles). This maxi-anion channel has a linear unitary current–voltage relationship without rectification and is prominently sensitive to the membrane potential, thereby rapidly inactivating when a threshold of ±20 to ±30 mV is exceeded. A macroscopic conductance with such a phenotype could readily be observed in whole-cell recordings from hypotonically swollen cells, when the VSOR activity was completely suppressed by its relatively specific inhibitor, phloretin, and when ATP was removed from pipette solution [8].

In our previous review article [10], we highlighted a newly discovered physiological role of maxi-anion channel in ATP release in response to osmotic stress in mammary C127 cells and in response to salt stress in tubuloglomerular feedback in kidney macula densa. Since then, we have carried out extensive studies on the maxi-anion channel along the following four lines: (1) its biophysical properties including the pore size [11], (2) its role in ATP release from astrocytes [6, 7] and cardiomyocytes [2, 12] under ischemic or osmotic stress, (3) its role in glutamate release from astrocytes under ischemic or osmotic stress [5], and (4) its molecular identification [13, 14]. The present review article, thus, gives an updated account of the biophysical properties, the roles in release of ATP and glutamate under pathophysiological conditions, and the molecular identification of the maxi-anion channel. Also, we intended to provide a comprehensive account of physiological and pharmacological characteristics of the maxi-anion channel in the present review, because it passed over a decade since a most recent comprehensive review on this channel was published by Strange et al. [15].

Expression pattern of the maxi-anion channel

The volume-activated large-conductance anion channels exhibiting properties typical of the maxi-anion channels have been found in different types of cell preparations. The single-channel event of large conductance was first described by Blatz and Magleby [16] in the plasma membrane patches excised from rat skeletal muscles in primary culture. About the same time, large-conductance channels with anion selectivity and bell-shaped voltage dependency were described in myotubes obtained from chicken embryos and in mouse peritoneal macrophages [17], in Schwann cells from 1 to 2 days old rats in primary culture [18] and in A6 *Xenopus* kidney epithelial cells [19]. Later, when a broader range of cell types was studied by patch-clamp technique, the activity of maxi-anion channels with a unitary conductance of 300–400 pS has been reported in almost every part of the whole organism. Maxi-anion channel activities have been found in freshly isolated frog *skeletal muscles* [20, 21], somatic muscles of *Ascaris suum* [22], as well as in cultured L6 rat muscle cells [23–26] and BC3H1 myoblasts [27]. *Smooth muscles* from uterus [28] and colon [29, 30] as well as cultured vascular smooth muscle cells from rat thoracic aorta [31–33] were found to express the maxi-anion channel activity. In the *heart*, maxi-anion channels were described in neonatal cardiac myocytes in primary culture [2, 12, 34, 35] and freshly isolated adult ventricular cardiomyocytes [12]. In the *nervous system*, the maxi-anion channel activity was detected in embryonic *Xenopus* spinal neurons [36], demyelinated *Xenopus* axons [37], in neuroblastoma cell lines [3, 38–44] and in a hippocampal cell line [45, 46]. In *glia*, maxi-anion channels were found in cultured Schwann cells from 1 to

2 day old rats [18] and adult humans [47] as well as in freshly dissected rat spinal root Schwann cells [48]. These channels were similar to those observed in cultured cortical astrocytes from rats [4, 49, 50] and mice [5–7, 51] as well as in a rat astrocytic RGCN cell line [52]. In *epithelia*, the urinary bladder [53], gastric [54], pancreatic [55–57], colonic [58–60], airway [61–63], choroid plexus [64], bile duct [65, 66], ciliary [67–69], renal [9, 19, 70–78], vestibular [79], placental [80–86], ruminal [87] and ovarian [84] epithelial cells were also found to express the maxi-anion channel with properties similar to those of excitable cells. Resembling maxi-anion channels were also found in *fibroblasts* [14, 66, 88–92] and *endothelial* cells [93–97]. In the *immune system*, the maxi-anion channel activity has been confirmed in B lymphocytes [98–101], in T lymphocytes [102–104] and in peritoneal macrophages [17, 105]. In other tissues, *mast* cells [106], *keratinocytes* [107], *osteogenic* cells [108], cultured glomus cells of the *carotid body* [109], PC12 *pheochromocytoma* cells [110], *pavement cells* from the gills of the trout [111] and *mammary* gland C127 cells [8, 11, 112] have also been shown to possess this channel. Patch-clamping the *intracellular organelles* revealed the maxi-anion channel activity in sarcoplasmic reticulum "sarcoballs" [113], whereas the presence of this channel in endoplasmic reticulum [114] and in Golgi complex [115] was demonstrated by reconstituting these membranes into liposomes and lipid bilayers, respectively. Thus, it is likely that the maxi-anion channel is widely expressed in almost every part of the body.

Studying the cardiomyocytes, we came across a puzzling observation that a high level of maxi-anion channel activity could be observed with primary cultured neonatal cells, but not with freshly isolated adult cardiomyocytes patched by a conventional patch-clamp technique [2, 34]. It was hypothesized that maxi-anion channels are only transiently expressed in neonatal cells, disappearing upon maturation [34]. However, ATP release from mature cardiomyocytes and purinergic signaling in the normal and diseased heart are well-recognized phenomena. We thus hypothesized that the difference in maxi-anion channel activity between neonatal and adult cells could be related to different pattern of spatial distribution of the maxi-anion channels over the surface of sarcolemma. When adult cardiomyocytes were patched using fine-tipped pipettes (15–20 MΩ), which were targeted to only Z-line areas, the maxi-anion events could be observed even in adult cells, as shown in Fig. 2. When different regions of the cell surface were subjected to excision and patch-clamp by using a recently developed "smart-patch" method [116–118], we found that the channel activity was maximal at the opening of T-tubules and along Z-lines, but was virtually absent in the scallop crest area [12], as shown in Fig. 2a. Even in the cell-attached configuration, unitary maxi-anion channel events were activated in adult rat cardiomyocytes by osmotic swelling after a lag time of around 9 min [12], as shown in Fig. 2b. Thus, it is concluded that maxi-anion channels do not disappear upon maturation, but become concentrated at the openings of T-tubules and along Z-lines in adult cardiomyocytes.

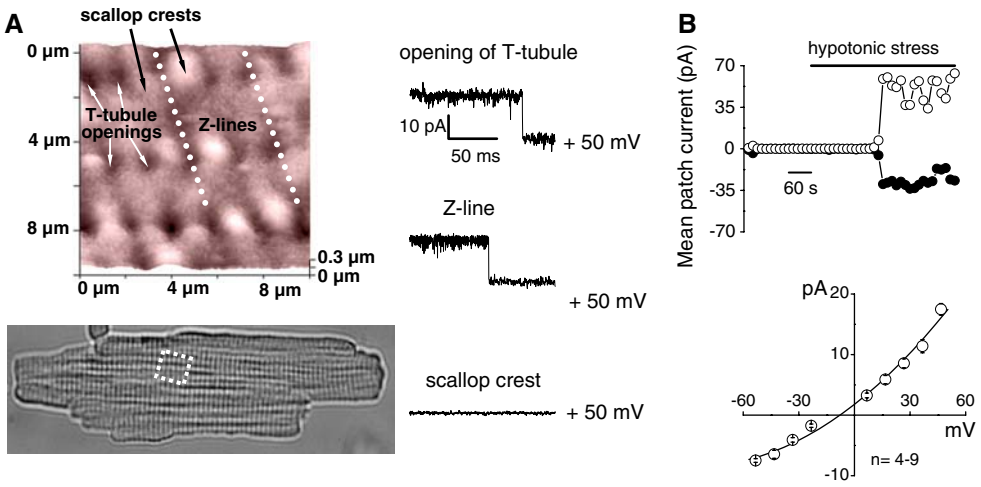

Fig. 2 Maxi-anion channel activity localized in specific regions on freshly isolated adult rat cardiomyocytes. **a** Topographic image of the area indicated by a white rectangle in the optical image shown at the bottom part on the surface of a cardiomyocyte obtained using scanning ion conductance microscopy (SICM) with a fine nanopipette. The maxi-anion channel activity in patches excised from Z-grooves, T-tubule openings, and scallop crests using the "smart-patch" technique are shown on the right side. **b** Swelling-induced activation of the maxi-anion channel activity in sarcolemma of adult cardiomyocytes. Mean patch currents recorded at +50 mV (*open circles*) and −50 mV (*filled circles*) in a cell-attached patch before and during (*horizontal bar*) exposure to hypotonic solution. Single-channel I–V relationship for these on-cell events is shown on the lower panel. Each symbol represents the mean ± SEM (*vertical bar*). Modified from Dutta et al. [12]

Basic biophysical properties of the maxi-anion channel

The maxi-anion channel exhibits roughly uniform behavior in different types of cells. Its very large single-channel conductance (300–400 pS) in physiological conditions distinguishes it from other chloride channels. Most authors noted that the maxi-anion channel has multiple subconductance states of various levels, such as ~15, ~50, ~100, ~150 and ~200 pS [2, 17, 29, 95]. When the ambient Cl^- concentration varied, the single-channel conductance saturated at 640 pS with $K_m = 112$ mM in L6 myoblasts [24], at 581 pS with $K_m = 120$ mM in T lymphocytes [104] and at 617 pS with $K_m = 77$ mM in frog skeletal muscle "sarcoballs" [113].

The current–voltage relationship of the fully open state is usually symmetrical and linear with no rectification (Fig. 1b, filled circles). The channel has a maximal open channel probability at around 0 mV, but readily closes when the voltage exceeds a range of ±15 to +30 mV (Fig. 3a). Thus, the macroscopic currents exhibit time-dependent inactivation at large positive and negative potentials over ±15 to +30 mV (Fig. 3b). Depending on cell types, such voltage sensitivity varies, and in some cases the channel has preferential gating by positive or negative potentials. However, the voltage dependence of open probability (P_{open}) remains bell-shaped with maximum at a certain voltage near 0 mV (Fig. 3c). The half-maximal open probability ($V_{1/2}$) was observed at −22.8 and +18 mV in normal T lymphocytes with effective gating charges of 5.7 and 9.6 for negative and positive voltages, respectively [104]. In cultured L6 myoblasts, the $V_{1/2}$ values were −25.6 and +49.6 mV for quiescent cells and −15.5 and +31.4 mV for rapidly proliferating cells [24]. The effective gating charge was dependent on cell growth and shifted from lower values for quiescent cells (3.5 and 1.7) to larger values for proliferating cells (10.6 and 3.7 at negative and positive voltages, respectively). Similar to T lymphocytes, a gating with higher $V_{1/2}$ at negative voltages compared to that at positive voltages (−36.9 vs. +13.9 mV) was reported for the maxi-anion channel in mammary C127 cells [8], as shown in Fig. 3c.

In many cell types, the maxi-anion channel can discriminate well for anions over cations. A high permeability ratio of chloride over sodium (P_{Cl}/P_{Na}) was reported for maxi-anion channel in bovine pigmented ciliary epithelial cells (24 [68]), T lymphocytes (30 [104]), neuroblastoma cells (30 [3]), in neonatal rat cardiac myocytes (24.6 [34]) and in mammary C127 cells (21–26 [8]). On the other hand, somewhat lower P_{Cl}/P_{Na} (6–11) was observed for human colonic HT-29 cells [58], freshly isolated guinea pig fetal type II alveolar epithelial

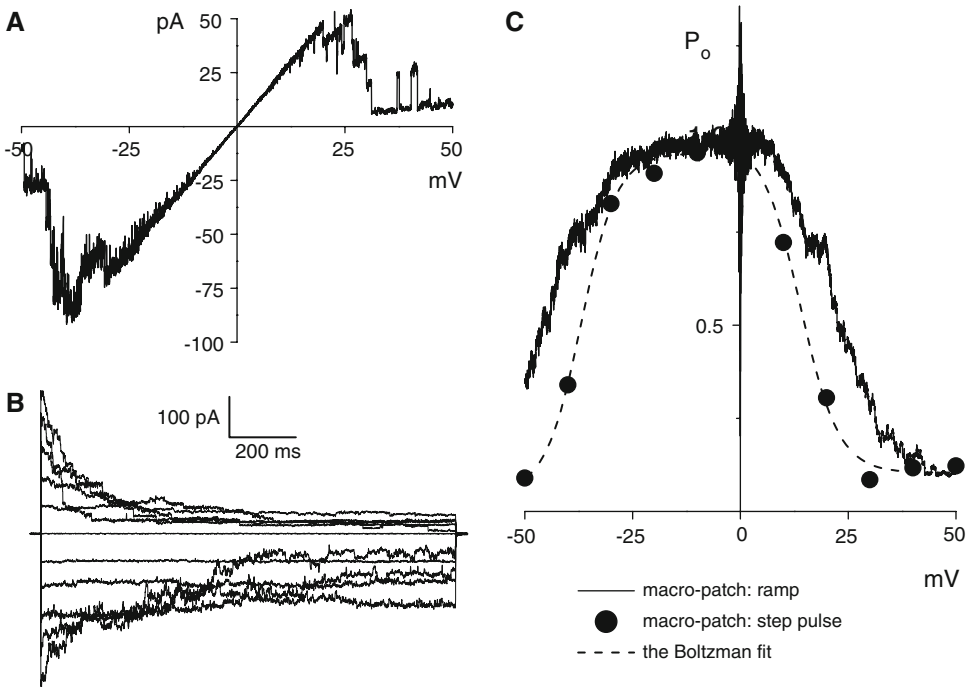

Fig. 3 Voltage-dependent inactivation of maxi-anion channel currents recorded in macro-patches excised from mammary C127 cells. **a** Steady-state ramp I–V records from a macro-patch containing five active channels. **b** Inactivating current traces recorded in response to step pulses from 0 to ±50 mV in 10-mV increments in a macro-patch containing 20 active channels. **c** Voltage dependence of steady-state open-channel probability. *Filled circles* represent the ratio of steady-state macro-patch current to instantaneous macro-patch current (from **b**). The Boltzmann fit (*dashed line*) yields a half-maximal open-channel probability at $V_{1/2} = +13.9$ and −36.9 mV for positive and negative potentials, respectively. The solid line is the ensemble-averaged current of 11 consecutive ramp-pulse records similar to those shown in (**a**). Modified from Sabirov et al. [8]

cells [61], rat bile duct epithelial cells [65], L6 rat muscle cells [24], and colonic smooth muscle cells [30]. Studying the maxi-anion channel of T lymphocytes, Schlichter et al. [104] found a decrease in anion selectivity from $P_{Cl}/P_{Na} = 30$ measured under balanced osmolarity to $P_{Cl}/P_{Na} = 11$ in the presence of osmotic gradient. These results indicate that the channel is highly selective to anions but the degree of anion selectivity may vary not only with cell types but also with the experimental conditions.

Selectivity data for different inorganic and organic anions are summarized in Table 1. In many cells, the selectivity of maxi-anion channels was found to follow the Eisenman's sequence I for weak electric field with permeability sequence of iodide > bromide > chloride > fluoride [8, 31, 33, 54, 58, 104]. The channel permits passage of large organic anions, including gluconate, glutamate, aspartate and lactobionate (Table 1). Hurnak and Zachar [25] studied the relationship between the minimum cross-sectional areas of the anions and their relative permeabilities and estimated the pore diameter of maxi-anion channel in cultured myoblasts to be approximately 0.6 nm. A similar estimate (pore radius of 0.32 nm) was obtained by Soejima and Kokubun [33] from the cross-sectional area of the largest tested anion, $HEPES^-$, permeability of which was already undetectable. In our study, analysis of the permeability of the maxi-anion channel in mammary C127 cells to organic anions of different sizes using the excluded area theory yielded a pore radius of 0.55 or 0.75 nm depending on whether or not frictional forces were taken into account [11]. However, comparison of permeability ratios with the electrical mobility ratios for the tested organic anions yielded a surprising linear relationship with a slope close to 1, when these

Table 1 Selectivity sequence and permeability ratios P_x/P_{Cl} (given in parenthesis) for maxi-anion channel of different types of cells

Cells	Selectivity sequence	References
Rat cultured Schwann cells	I^- (1.4) > Br^- (1.2) > Cl^- (1.0) > methyl-SO_4^- (0.72) > SO_4^{2-} (0.61) > acetate$^-$ (0.39) = isethionate$^-$ (0.39) > aspartate$^-$ (<0.03), glutamate$^-$ (<0.03)	Gray et al. [18]
Rabbit urinary bladder epithelial cells	Cl^- (1.0) ≈ Br^- (1.0) ≈ I^- (1.0) ≈ SCN^- (1.0) ≈ NO_3^- (1.0) > F^- (0.57) > acetate$^-$ (0.30) > gluconate$^-$ (0.07)	Hanrahan et al. [53]
Rat cultured pulmonary alveolar (type II) cells	I^- (1.5) > Br^- (1.02) ≥ Cl^- (1.00) > NO_3^- (0.9) > gluconate$^-$ (0.6)	Schneider et al. [63]
Rat cultured smooth muscle cells from embryonic aorta	I^- (1.4) > Br^- (1.3) > Cl^- (1.0) > F^- (0.7)	Soejima and Kokubun [33]
Rat cultured glomus cells of the carotid body	Cl^- (1.0) > HCO_3^- (0.71) > SO_4^{2-} (0.57) > glutamate$^-$ (0.14)	Stea and Nurse [109]
Mouse B lymphocyte-myeloma hybridoma cells	F^- (1.25) > I^- (1.18) > SCN^- (1.10) > Br^- (1.07) > Cl^- (1.00) > glucuronate$^-$ (0.78) > NO_3^- (0.68) > aspartate$^-$ (0.62)	Bosma [98]
Human T lymphocytes	I^- (1.38) > NO_3^- (1.14) > Br^- (1.04) > Cl^- (1.0) > F^- (0.57) > SCN^- (0.56) > HCO_3^- (0.56) > SO_4^{2-} (0.49) > gluconate$^-$ (0.29) ≈ propionate$^-$ (0.30) > aspartate$^-$ (0.08)	Schlichter et al. [104]
Chick cultured embryonic osteogenic cells	Cl^- (1.0) > methylsulfate$^-$ (0.71) > gluconate$^-$ (0.25) > glutamate$^-$ (0.17)	Ravesloot et al. [108]
Human colon carcinoma HT-29cl.19A cells	I^- (1.2) > Br^- (1.05) > Cl^- (1.0) > F^- (0.46) > gluconate$^-$ (0.24)	Bajnath et al. [58]
Ascaris suum muscle membrane vesicles	I^- > Br^- = NO_3^- > Cl^- > F^-	Dixon et al. [22]
Rat muscle L6 cells	Br^- (1.18) > I^- (1.15) > NO_3^- (1.13) > Cl^- (1.0) > methanesulfonate$^-$ (0.60) > HCO_3^- (0.59) > propionate$^-$ (0.44) > SO_4^{2-} (0.40) > glutamate$^-$ (0.1)	Hurnak and Zachar [25]
Guinea-pig parietal cells	I^- > Br^- > Cl^- > F^-	Kajita et al. [54]
Mouse mammary C127 cells	I^- (1.31) > Br^- (1.14) > Cl^- (1.0) > F^- (0.61) > phosphate^{2-} (0.43) > aspartate$^-$ (0.23) ≈ glutamate$^-$ (0.22)	Sabirov et al. [8]
Mouse mammary C127 cells	Cl^- (1.0) > formate$^-$ (0.66) > pyruvate$^-$ (0.52) > methanesulfonate$^-$ (0.51) > acetate$^-$ (0.50) > propionate$^-$ (0.39) > glucuronate$^-$ (0.19) > glucoheptonate$^-$ (0.18) > gluconate$^-$ (0.17) > glutamate$^-$ (0.16) > lactobionate$^-$ (0.13)	Sabirov and Okada [11]

ratios were plotted against each other. This result suggests that even large anions move inside the maxi-anion channel pore by free diffusion with little or no interference by the pore wall. Thus, pore size values based on ionic permeability measurements are underestimated. In fact, using non-charged polymeric molecules as a probe, we obtained larger estimates of the maxi-anion channel pore size, as shown in Fig. 4. Thus, one-sided application of polyethylene glycols (PEGs) yielded an effective pore radius of 1.16 and 1.42 nm for cytosolic and extracellular entrances, respectively [11], whereas two-sided application of PEGs gave an averaged radius of ~1.3 nm (Fig. 4). This result is in contrast to the pore radius similarly estimated for a volume-activated anion channel, VSOR (0.6 nm: [119]) and a cAMP/PKA-activated anion channel, CFTR (0.6–1.0 nm: [120]). The pore size of maxi-anion channel thus largely exceeds the size of small organic anions (e.g. 0.35 nm for glutamate) and is sufficient for transport of larger organic anions (e.g. 0.58–0.65 nm for ATP: Fig. 4).

The maxi-anion channel in gastric parietal cells was insensitive to extracellular pH 5–8 [54]. In cultured glomus cells of the rat carotid body the channel was insensitive to the intracellular pH 6.5–8 in inside-out patches [109]. However, high external pH 9 shifted voltage dependence of the maxi-anion channel to more negative values in frog skeletal muscles [21]. For the tracheal maxi-anion channel reconstituted into giant liposomes, low bath pH reduced channel open probability in inside-out patches yielding an apparent pK of 6.09 [57]. However, the channel current amplitude did not change with acidification suggesting that the protonation site is located far from the channel permeation pathway.

Pharmacological properties of the maxi-anion channel

Similar to other chloride channels, the maxi-anion channel was found to be suppressed, though not completely, by classical anion channel blockers, such as NPPB and SITS (Fig. 5) as well as DIDS and DPC [2, 5, 6, 8, 12, 30, 54, 93, 96, 103, 114]. However, maxi-anion channels were found to be completely insensitive to phloretin, which is a relatively specific blocker for VSOR [121], in mouse mammary C127 cells [8, 112] and mouse astrocytes [5, 6, 8, 112], and to glibenclamide (Fig. 5), which blocks not only CFTR but also VSOR [122], in mouse C127 cells [8], rat cardiomyocytes [2] and mouse astrocytes [5]. An anion channel inhibitor, L-644-711 (0.5–1 mM), also blocked maxi-anion channels in cultured rat astrocytes [4]. Arachidonic acid at a micromolar level inhibited maxi-anion channels in an L6 rat muscle cell line [26], from human term placentas membranes reconstituted into giant liposomes [84], in mouse mammary C127 cells [112], in cultured neonatal rat cardiomyocytes [2, 12] (Fig. 5), in primary cultured mouse astrocytes [5, 6], and in primary cultured mouse fibroblasts [14], whereas the gastric endothelin-activated maxi-anion channel was insensitive to arachidonic acid added from outside [54]. Dutta et al. [112] found that the maxi-anion channel of mammary C127 cells was inhibited by arachidonic acid in two different ways: channel shutdown (K_d of 4–5 μM) and reduced unitary conductance (K_d of 13–14 μM) without affecting voltage dependence of open probability. The negative charge and *cis*-conformation of the arachidonate are essential for the channel inhibition,

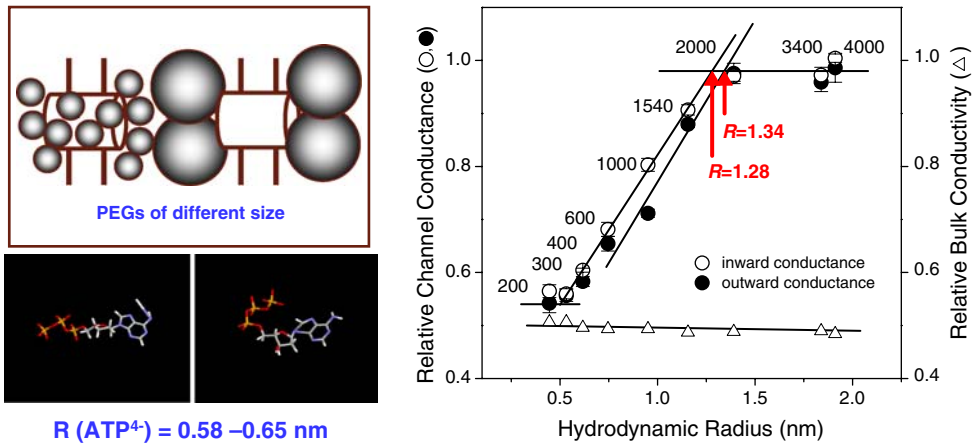

Fig. 4 Maxi-anion channel has a wide pore larger than the size of ATP. *Left panels* Basic principle of the polymer partitioning method using PEGs (depicted as globules) of different sizes (*upper panel*) and the effective pore radius (R) of an ATP molecule calculated in two different conformations: conventional long and more compact forms found in crystals (see for details: Sabirov and Okada [11]). *Right panel* Relative single maxi-anion channel conductance (*circles*) and relative bulk solution conductivity (*triangles*) as a function of the hydrodynamic radius of PEGs. Each symbol represents the mean ± SEM (*vertical bar*) ($n = 5$–20). Pore size is estimated as an intersection point between a rising portion of the curve (partial partitioning) and an upper plateau level (complete exclusion). Modified from Sabirov and Okada [11]

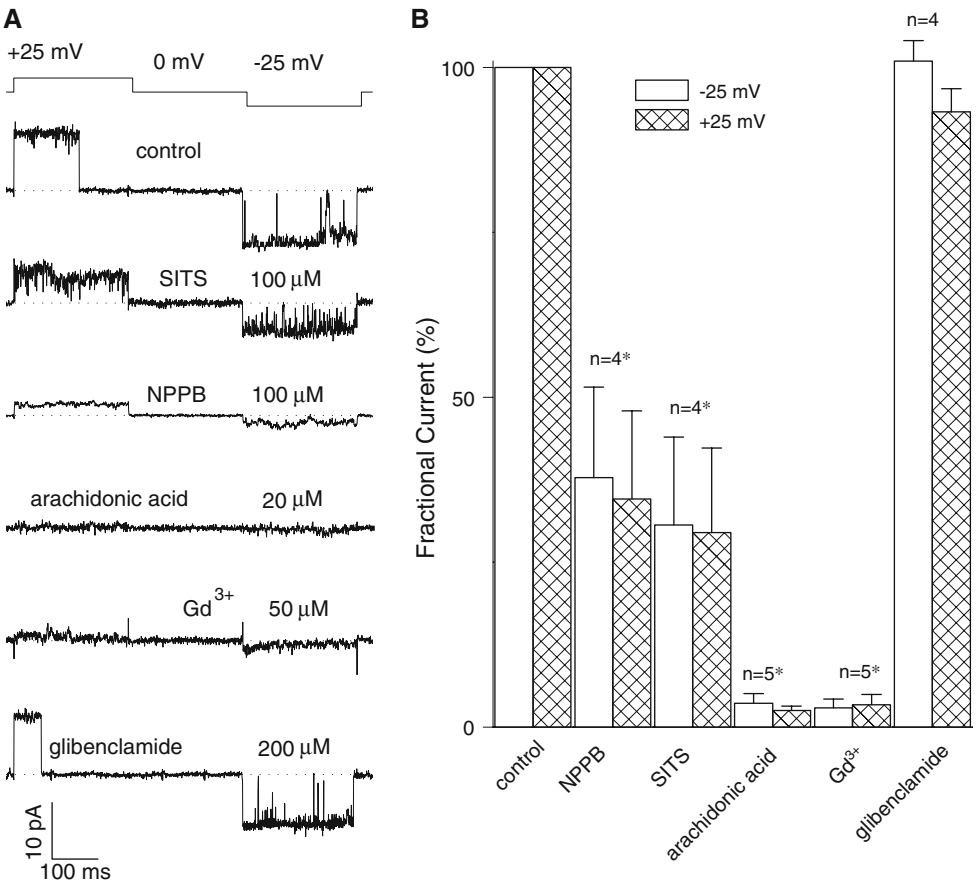

Fig. 5 Pharmacological profile of the maxi-anion channel in primary cultured neonatal rat cardiomyocytes. **a** Single-channel current traces recorded from excised outside-out (for Gd^{3+}) and inside-out (for others) patches during application of step pulses (the protocol shown at the top of traces) in the absence (control) or presence of drugs. **b** Effects of drugs on mean currents recorded from excised macro-patches. Currents were recorded at +25 mV (*open columns*) and −25 mV (*hatched columns*). Data are normalized to the mean current measured before application of drugs and after correction for the background current. Each column represents the mean ± SEM (*vertical bar*). $*P < 0.02$ versus control. Modified from Dutta et al. [2]

which occurs from the intracellular, but not extracellular, side [109].

Gadolinium ions are considered as a relatively selective inhibitor of the stimulated ATP release [123, 124]. Gd^{3+} at the concentration of 30–50 µM effectively shuts down the maxi-anion channels from the extracellular (Fig. 5), but not the cytosolic, side [2, 5, 6, 8, 12, 14]. This is in contrast to the VSOR which is insensitive to gadolinium ions [8, 125]. Zn^{2+} ions also effectively blocked the maxi-anion channel both from extra- and intracellular sides in different cell types [26, 31, 93, 103, 111].

In mouse N1E 115 neuroblastoma cells, a type II pyrethroid, deltamethrin, at micromolar concentrations inhibited the maxi-anion channel activity [43], whereas ivermectin (10^{-7} M) and pentobarbitone (10^{-6} M) significantly increased open channel probability [44].

Activation of the maxi-anion channel by physiological/pathophysiological stimuli

Although the maxi-anion channel activity is rarely seen in cell-attached patches on resting cells, the channels can be activated by variety of physiologically/pathophysiologically relevant stimuli. As summarized in our previous review [10], the maxi-anion channel is activated by osmotic *cell swelling* in cortical collecting duct (CCD) cells [9], neuroblastoma cells [3], cortical astrocytes in primary culture [4, 5], mammary C127 cells [8, 112] and in cardiomyocytes [2, 12] (Fig. 6a). In cardiomyocytes [2, 12] (Fig. 6b, c) and astrocytes [2, 5, 6, 12], the channel is also activated in response to the chemical *ischemia* and *hypoxia*. In kidney macula densa cells, the channel becomes activated in response to *salt stress*, namely reduction of the NaCl concentration in the tubular fluid [70]. Maxi-anion channels could be activated by *endothelin-1* via EB-receptor during whole-cell recordings from guinea-pig parietal cells [54]. In cell-attached patches, the maxi-anion channels were activated by an agonist of *A1-adenosin receptor*, N^6-cyclohexyladenosine, in cortical collecting duct cells [75] and by *bombesin*, a Ca-mobilizing peptide mitogen, in Swiss 3T3 fibroblasts [90]. On NIH3T3 fibroblasts and porcine aortic endothelial cells, both grown in the presence of colchicines, the maxi-anion channels were activated by extracellularly added *antiestrogens*, toremifene [89] and tamoxifen [94]. The effect could be blocked by 17β-estradiol but not by progesterone. A similar effect of these antiestrogens on C1300 neuroblastoma cells was blocked by okadaic acid, suggesting a role of Ser/Thr phosphorylation in this process [42]. Henriquez and

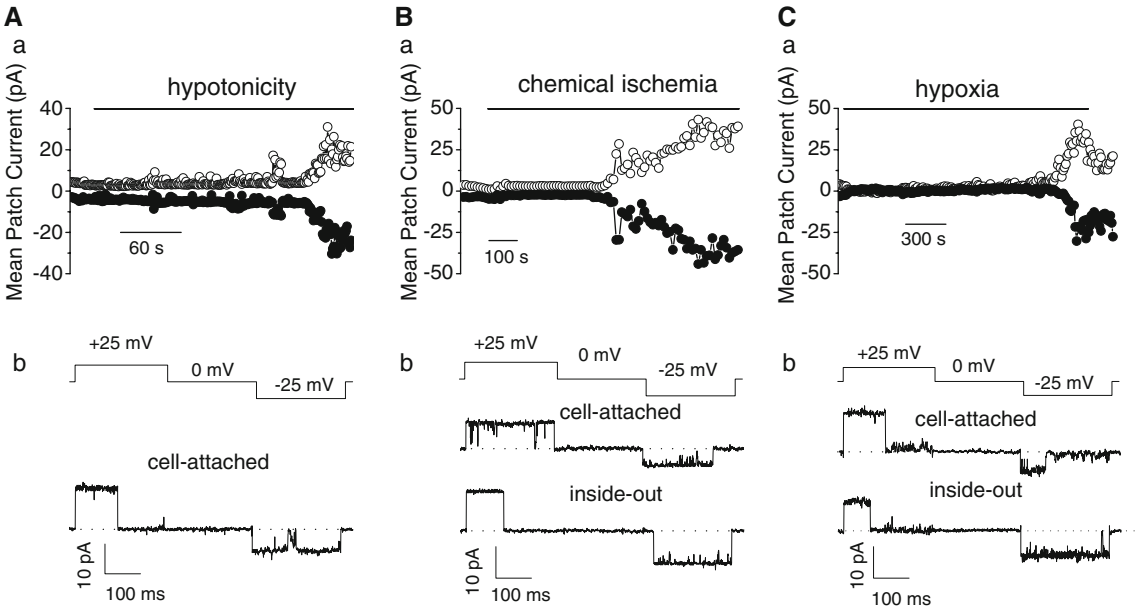

Fig. 6 Maxi-anion channel activation upon hypotonic (**a**), ischemic (**b**) and hypoxic (**c**) stresses in neonatal rat cardiomyocytes. *a* Mean patch currents during application of alternating pulses from 0 to ±25 mV in a cell-attached patch before and during (*horizontal bar*) exposure to hypotonic, ischemic or hypoxic solution. *b* Representative current traces of maxi-anion channels activated as in (*a*) and elicited by step pulses of ±25 mV (the protocol shown at the top of traces) in cell-attached or inside-out patches. Modified from Dutta et al. [2]

Riquelme [82] reported a direct modulation by 17β-estradiol and tamoxifen of the maxi-anion channel from human placenta reconstituted into giant liposomes. *Bradykinin* and an NK-1 receptor antagonist, *substance P methylester*, were also able to activate the maxi-anion channels in cell-attached patches on pig aortic endothelial cells [93] and rabbit colonic smooth muscle [29, 30], respectively. Interestingly, the channels could be reversibly activated by raising the ambient *temperature* above 32°C both in cell-attached and whole-cell experiments in human T lymphocytes [103]. In several studies, a strong stimulus to activate the maxi-anion channel was *patch excision* (see [15]).

Obviously, a very strict regulatory system controls the channel physiological state, which provides a low basal activity of maxi-anion channel in resting conditions. The mechanism of the maxi-anion channel activation by cellular swelling remains poorly understood at present. Hypoosmotic stress is known to activate several signaling pathways [1, 126, 127], which are also involved in the maxi-anion channel regulation. These include protein phosphorylation, changes in the intracellular concentration of Ca^{2+} and cAMP, G proteins, membrane stretch and cytoskeleton, and so on. Intracellular regulatory pathways involved in maxi-anion channel regulation were studied in a number of cell types. Thus, intracellular signaling via PKA and PKC phosphorylation has been suggested to regulate the maxi-anion channel in rabbit cortical collecting duct cells [9], bovine aortic endothelial cells [97], pig aortic endothelial cells [93], and rat vascular smooth muscle cells [31, 32]. Meanwhile, in rabbit colonic smooth muscle cells, PKA and PKC inhibitors had no effect on the maxi-anion channel activity [29]. The channel was shown to be regulated by G proteins: the channels were activated by GTPγS and inhibited by GDPβS and pertussis toxin (PTX) in rabbit renal cortical collecting duct cells [75, 76] and in rabbit colonic smooth muscle cells [29]. However, an opposite type of regulation was observed in rat bile duct epithelial cells, where PTX and GDPβS activated, whereas GTPγS inhibited the maxi-anion channels [65, 66], suggesting a cell-specific channel regulation by G proteins.

Activation of maxi-anion channels upon patch excision may imply an involvement of the cytoskeleton in the maxi-anion channel regulation. Indeed, in cortical collecting duct cells, Schwiebert et al. [9] demonstrated that in inside-out patches, the maxi-anion channel could be activated by disruption of F-actin using dihydrocytochalasins. Short actin filaments activated the channels, whereas long actin filaments inhibited, and 1 mM ATP reversed effect of dihydrocytochalasin B. In addition, phalloidin abolished the channel activation by negative pressure [9]. Mills et al. [128] proposed that swelling-induced membrane stretch activates the maxi-anion channel by a mechanism, which involves fragmentation and depolymerization of F-actin.

Although most authors found that maxi-anion channels are insensitive to changes in the cytosolic free Ca^{2+} concentration in excised inside-out patches, elevation of cytosolic Ca^{2+} by a Ca-ionophore, A23187, was found to increase the incidence of channels in the cell-attached

mode in human colonic cells HT-29 [58], Swiss 3T3 fibroblasts [90], pig aortic endothelial cells [93] and embryonic *Xenopus* spinal neurons [36].

On balance, it must be stated that available data are still fragmentary to deduce the precise mechanisms of activation of the maxi-anion channel. Also, studies for the molecular mechanisms have been largely hampered by the lack of molecular identification of this channel.

Hypothesized roles of the maxi-anion channel in the Cl^- transport

As an electrogenic chloride-transporting pathway, the maxi-anion channel has been implicated in a number of physiological functions, which involve Cl^- movement. Thus, the channel was deemed to provide a rout for solute transport and/or bicarbonate secretion in pancreatic duct cells [55], in alveolar epithelium [63], in syncytiotrophoblasts of placenta [83, 129], in sheep ruminal epithelium [87] and in glomus cells of the rat carotid body [109]. The channel is thought to participate in the Cl^- efflux during cell volume regulation in cortical collecting duct epithelium [9, 75], pigmented ciliary epithelial cells [68], lymphocytes [102, 104], myoblasts [23], placenta [80], neuronal cells [3] and astrocytes [4]. The maxi-anion channel is expressed in the ciliary epithelium, where it may participate in the aqueous humor secretion [67, 130], and in the hepatic bile duct, where it could be involved in bile formation [65, 66]. Efflux of Cl^- ions during apoptotic cell shrinkage is also thought to occur via maxi-anion channels in neuronal cells [46]. Chloride influx as a counter ion for potassium uptake is thought to be a function for the maxi-anion channel in Schwann cells [47, 48]. The maxi-anion channel may also be involved in regulating charge balance and membrane potential of the Golgi complex by providing a counter anion pathway for the H^+-ATPase [115]. Regulation by estrogens and antiestrogens links the maxi-anion channel to the intracellular signaling pathways of the cells expressing estrogen receptors [42, 89]. A possible role in signal transduction in B cell activation [99, 100] and in receptor-mediated initial cell depolarization in colonic smooth muscle cells [29] has also been proposed.

It should however be noted that in most papers, the proposed physiological roles are mainly hypothetical without making critical comparison of pharmacology between the proposed functions and the maxi-anion channel.

Roles of the maxi-anion channel in stimulated release of ATP and glutamate

Adenosine-5′-triphosphate (ATP) is not only a universal energy source constantly produced and utilized by cells at high rates, but it also serves as an "extracellular second messenger" for autocrine and paracrine signaling at cellular as well as tissue/organ levels [131–135]. When cells are stimulated, they release small amounts of this signalling molecule, which then binds to P2 purinergic receptors expressed in virtually all cell types [136]. ATP is a relatively large and hydrophilic molecule, and it needs specially designed pathways in order to exit the cells. Most ATP molecules and its complex with Mg^{2+} exist in the cytoplasm in anionic forms at physiological pH ($\sim$87% as $MgATP^{2-}$ and $\sim$11% as ATP^{4-}: see [137]. Therefore, it is possible that an anion channel can electrogenically translocate ATP^{4-} or $MgATP^{2-}$, thereby serving as a conductive pathway for ATP release (see for review [10, 137]). The maxi-anion channel is a very likely candidate for this role due to the following five reasons: (1) The stimuli, which effectively activated the maxi-anion channel, also produced a massive release of ATP. This has been confirmed in mammary C127 cells [8], cardiomyocytes [2, 12] and astrocytes [6, 7] for osmotic stress; in kidney macula densa cells for the salt stress [70]; and in cultured neonatal [2] and acutely isolated adult cardiomyocytes [12] as well as in primary cultured astrocytes [6, 7] for the ischemic and hypoxic stresses. (2) In all these studies, the inhibitors of the maxi-anion channel, such as SITS, NPPB and Gd^{3+}, effectively suppressed the stimulated ATP release, whereas blockers of VSOR, phloretin and glibenclamide, had no notable effect on the stimulated release of ATP from the cells tested in these studies. (3) Our biophysical analysis showed that the maxi-anion channel is well suited for the function of a conduit for ATP^{4-} or $MgATP^{2-}$. Thus, ATP^{4-} added either from the extracellular or from the intracellular side produced a profound fast open-channel voltage-dependent blockage, revealing a weak ATP-binding site with K_d of 12–13 mM located approximately in the middle of the channel pore [8]. Pore-sizing experiments with polyethylene glycols indicated that the maxi-anion channel has a relatively large pore with an effective radius of $\sim$1.3 nm [11]. Such a wide nanoscopic pore provides sufficient room to accommodate ATP^{4-} or $MgATP^{2-}$, the radii of which are in the range of 0.6–0.7 nm (see [11]). (4) Replacing all the anions in the intracellular side with 100 mM ATP^{4-}, we were actually able to detect small inward currents carried by the nucleotide (Fig. 7a), which reversed at around -20 mV and yielded the permeability ratio P_{ATP}/P_{Cl} of $\sim$0.1 for the maxi-anion channels in all the cell types tested, including C127 cells [8, 112], macula densa [70], cardiomyocytes [2, 12] and astrocytes [6]. The maxi-anion channel was permeable also for $MgATP^{2-}$ (Fig. 7b) with the permeability ratio P_{MgATP}/P_{Cl} of $\sim$0.16 [2]. The maxi-anion channel does not discriminate well between the nucleotides and is permeable also to ADP^{3-} ($P_{ADP}/P_{Cl} = 0.12$) and

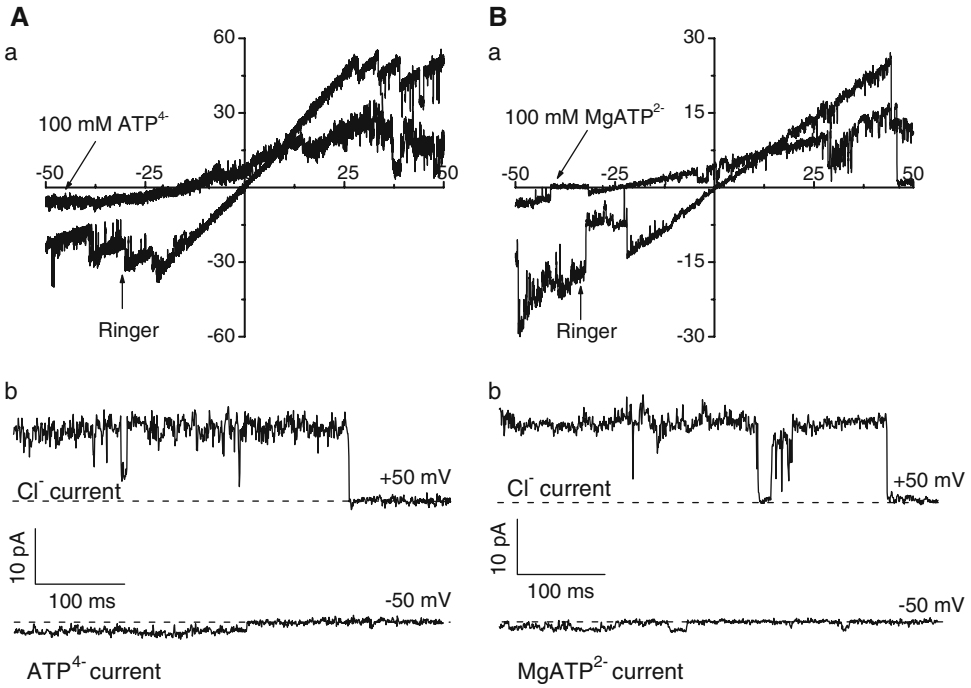

Fig. 7 ATP currents through the maxi-anion channel recorded in inside-out patches excised from neonatal rat cardiomyocytes. **a** Representative ramp I–V records (*a*) and channel activity in response to step pulses (*b*) from a macro-patch exposed to standard Ringer solution and one exposed to 100 mM Na_4ATP solution. The pipette solution was standard Ringer. **b** Representative ramp I–V records (*a*) and channel activity in response to step pulses (*b*) from a macro-patch exposed to standard Ringer solution and one exposed to 100 mM Na_2MgATP solution. The pipette solution was TEA-Cl. Modified from Dutta et al. [2]

UTP^{4-} ($P_{UTP}/P_{Cl} = 0.09$) [137]. The ATP currents were sensitive to the blockers of the maxi-anion channel, SITS, NPPB, Gd^{3+} [8] and arachidonic acid [112]. (5) Finally, recent studies by using a smart-patch technique [138] combined with a biosensor ATP detection technique [139, 140] demonstrated that the spatial distribution of the maxi-anion channel expression on the cell surface of both neonatal and adult rat cardiomyocytes coincides with that of the ATP releasing sites [12]. From these studies, the maxi-anion channel emerges as an important gateway for the purinergic cell-to-cell signaling providing an electrogenic conductive pathway for the translocation of ATP^{4-} and $MgATP^{2-}$ from the cytosol to the extracellular milieu. It is proposed that the maxi-anion channel-mediated release of ATP in response to salt stress is a central event during cell-to-cell communication between macula densa cells and mesangial cells, which express $P2Y_2$ receptors [70, 141]. This mechanism may represent a new paradigm in cell-to-cell paracrine signal transduction mediated by ATP in tubuloglomerular feedback [10, 141, 142]. In cardiac cells, the maxi-anion channel is suggested to play a protective role by releasing ATP during ischemic preconditioning [2, 12]. Astrocytes may communicate with neurons by releasing extracellular signaling molecules called gliotransmitters such as ATP and glutamate [143, 144]. Thus, it is suggested that purinergic cell-to-cell signaling in the brain occurs via activation of maxi-anion channels [5–7].

Astrocytes can also release their intracellular glutamate in physiological conditions in response to ATP, glutamate, bradykinin and prostaglandin E2 [145]. High levels of the extracellular glutamate of about 200–300 μM [146] can be observed during brain ischemia-reperfusion, and this released glutamate is considered as a main cause of brain excitotoxicity and neurodegeneration [147–149]. As shown in Fig. 8a–c, the astrocytic maxi-anion channel was found to be conductive to glutamate with $P_{glutamate}/P_{Cl}$ of 0.20 [5] and could, therefore, serve as a mediator for the stimulated glutamate release from cultured astrocytes. Consistent with this hypothesis, the swelling- and ischemia-induced release of glutamate was greatly suppressed by blockers of maxi-anion channels, such as NPPB, SITS, Gd^{3+} and arachidonate [5]. However, even a strongest inhibitor of the maxi-anion channel, Gd^{3+}, inhibited only about half of the total glutamate release in hypotonic conditions and about one-third of it under the chemical ischemia, as summarized in Fig. 8d, suggesting that an additional pathway is involved in the observed release of glutamate. This second pathway is likely to be the another volume-activated anion channel VSOR, because this channel is also permeable to glutamate with a permeability ratio $P_{glutamate}/P_{Cl}$ of 0.15 [5], and because the massive release of glutamate was partially suppressed by blockers of VSOR, phloretin and tamoxifen (Fig. 8d). Thus, it appears that both VSOR and maxi-anion channels jointly represent major conductive pathways for the release of glutamate from swollen and ischemia-challenged astrocytes with predominant contribution of the maxi-anion channel.

It is clear that the maxi-anion channel conducts $glutamate^{-}$, ATP^{4-} and $MgATP^{2-}$. What is, however, the number of active channels that would be sufficient for the observed net release of glutamate and ATP? Previously our quantitative analyses of the channel's conductance and the

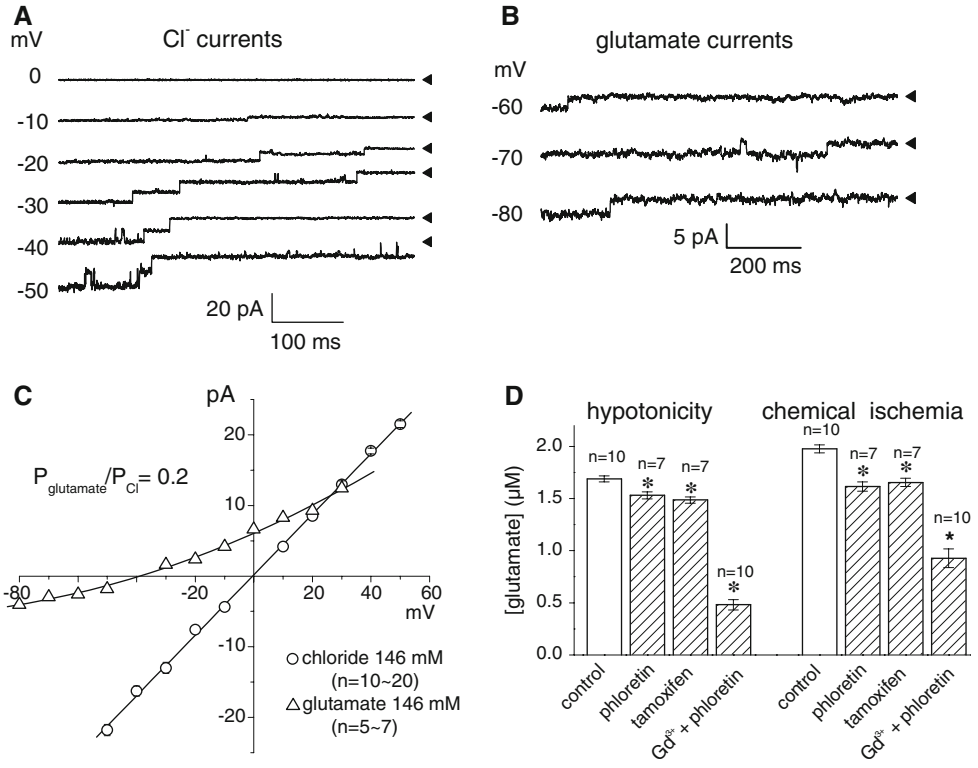

Fig. 8 Glutamate permeability of the glial maxi-anion channel and the pharmacological profile of the net glutamate release from astrocytes in hypotonic or ischemic conditions. **a** chloride currents recorded in symmetric conditions with both pipette and bath containing normal Ringer solution (146 mM Cl^-). **b** Glutamate currents through an astrocytic maxi-anion channel. Traces were recorded in asymmetrical conditions in which all chloride in the bath (intracellular) solution was replaced with 146 mM glutamate. Arrowheads indicate the zero current level. **c** Unitary I–V relationships for the maxi-anion channel in symmetrical chloride conditions (*open circles*) and in asymmetrical conditions in which all chloride in the bath (intracellular) solution was replaced with 146 mM glutamate (*open triangles*). Each symbol represents the mean (the error bar is smaller than the symbol size). The slope conductance for symmetrical conditions is 403.9 ± 1.7 pS. The solid line for asymmetrical conditions is a polynomial fit with a reversal potential of −38.9 ± 1.2 mV for 146 mM glutamate. **d** Effects of phloretin (100 μM), tamoxifen (50 μM) and Gd^{3+} (50 μM) plus phloretin (100 μM) on the net release of glutamate from astrocytes induced by hypotonic or ischemic stimulation (for 15 min). Each column represents the mean ± SEM (*vertical bar*). $^*P < 0.05$ compared with control. Modified from Liu et al. [5]

observed net release of these molecules suggested that brief opening of only a few maxi-anion channels would be sufficient to provide physiologically significant extracellular signals caused by the release of glutamate from cortical astrocytes [5] and that of ATP from cardiac myocytes [2].

The fact that the maxi-anion channel is blocked by ATP at millimolar range (see above) would suggest that some other intracellular anions (e.g. free amino acids or glycolysis intermediates) could also interact with the maxi-anion channel pore in vivo and interfere with the ionic fluxes. Although we did not detect any effect of glutamate on the channel amplitude up to 30 mM [5], we suppose that, in general, the fraction of the maxi-anion channels contributing to the release of ATP and/or glutamate could vary as a function of the concentrations of cytosolic constituents, which interact with the channel, depending on the intracellular state of the concerned cells.

Puzzle of the molecular identity of the maxi-anion channel

The molecular identity of the maxi-anion channel is not yet firmly established. As we described above, the maxi-anion channel has a very large single-channel conductance and bell-shaped voltage-dependent inactivation with maximal open probability at around 0 mV. These biophysical properties are similar to those of the voltage-dependent anion channel (VDAC, also called porin) expressed in the outer membrane of mitochondria [150–152]. Therefore, it has been widely held that VDAC located in the plasma membrane (pl-VDAC) is the most likely candidate protein [38, 45, 46, 49, 88, 110]. This hypothesis has received a great attention and considered to be an established concept in the field. Consistent with this idea, several groups have indeed reported the presence of VDAC protein in the plasma membrane of various cells [38, 49, 88, 110,

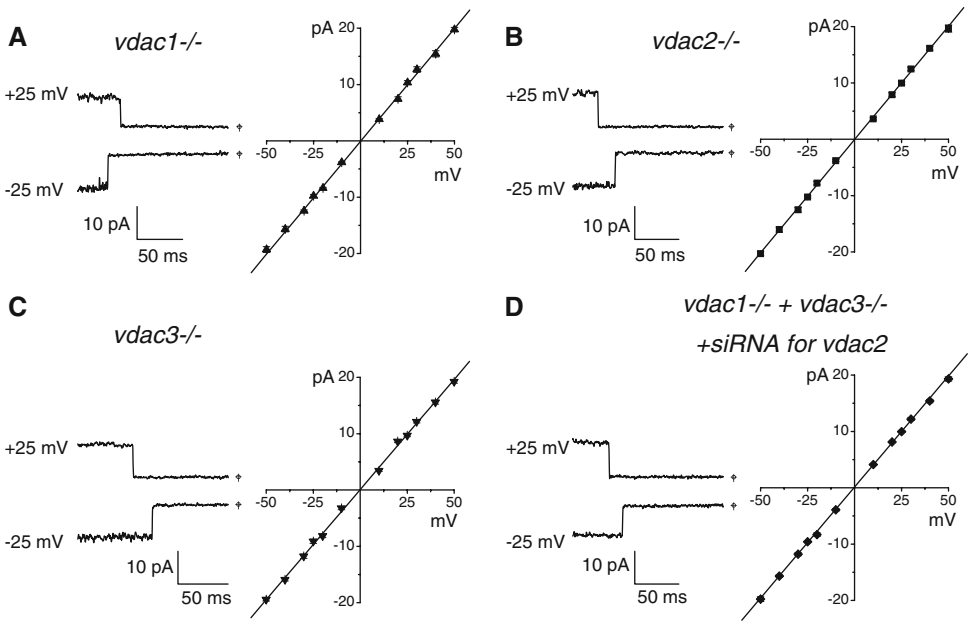

Fig. 9 Maxi-anion channel activities in VDAC-deficient fibroblasts. **a**, **b**, and **c** The channel activities in the cells derived from VDAC1-, VDAC2-, and VDAC3-knockout (*vdac1*$^{-/-}$, *vdac2*$^{-/-}$, and *vdac3*$^{-/-}$) mice, respectively. **d** The channel activity in the cells derived from VDAC1/VDAC3 double-knockout mice with the *vdac2* gene silenced by RNA interference. *Left panels* The representative current traces recorded at ±25 mV. *Right panels* The respective single-channel current-to-voltage (I–V) relationships. Each symbol represents the mean ± SEM (*vertical bar*) (n = 5–17). Modified from Sabirov et al. [14]

153–161]. A possible mechanism for targeting of the same protein to such different locations as mitochondria and the plasma membrane has been suggested by Buettner et al. [110]. These authors identified an alternative first exon in the murine *vdac1* gene that encodes a leader peptide at its N-terminus. This peptide serves as a signal to target the protein to the plasma membrane via Golgi apparatus and it is eventually cleaved away to produce a pl-VDAC protein identical to the mitochondrial one. Another mechanism involving mRNA untranslated regions has also been considered [162]. Three isoforms of mitochondrial porin, VDAC1, VDAC2 and VDAC3, have been cloned in mammals [49, 163–170]. If the maxi-anion channel is a pl-VDAC, then deletion and/or silencing of the VDAC genes would be expected to eliminate the channel activity. In order to test the "maxi-anion channel = pl-VDAC" hypothesis, we have deleted each of the three genes encoding the VDAC isoforms individually and collectively and demonstrated that maxi-anion channel (~400 pS) activity in VDAC-deficient mouse fibroblasts was unaltered [14]. Essentially similar maxi-anion channel activities were observed in mouse embryonic fibroblasts (MEFs) derived from VDAC1-, VDAC2- and VDAC3-deficient (*vdac1*$^{-/-}$, *vdac2*$^{-/-}$, *vdac3*$^{-/-}$) mice, as shown in Fig. 9a–c, as well as in MEFs from wild-type mice and in mouse adult fibroblasts (MAFs) from VDAC1/VDAC3 double-knockout mice [14]. As shown in Fig. 9d, the channel activity was also similar in VDAC1/VDAC3 double-deficient cells with the VDAC2 protein depleted by siRNA [14]. Thus, the lack of correlation between VDAC protein expression and maxi-anion channel activity strongly argued against the long held hypothesis of plasmalemmal VDAC being maxi-anion channel, but indicate that none of the three individual isoforms of VDAC can be responsible for the maxi-anion channel. The plasmalemmal VDAC proteins may perform some other functions, such as being a receptor for plasminogen kringle 5 [171] or a trans-plasma membrane NADH-ferricyanide reductase [172], activities that are unrelated to the maxi-anion channel activity.

It should be noted that the similarities in single-channel properties between the maxi-anion channel and VDAC are rather superficial, and closer inspection reveals very important differences, as summarized in Table 2. For instance, the VDAC single-channel conductance may reach levels of over 10 nS at high salt concentrations without any saturation [173], whereas the single-channel conductance of max-anion channel saturates at 580–640 pS with K_m of 77–120 mM [24, 104, 113]. The ability to discriminate between cations and anions is also very different between VDAC and maxi-anion channels: under the same 10-fold KCl gradient, the maxi-anion channel generated a reversal potential of about 40 mV [89], whereas no more than approximately 10 mV was observed for the mitochondrial VDAC [174], indicating that the maxi-anion channel is much more selective for chloride over potassium than the mitochondrial VDAC. Although the overall ranking of anionic permeability was similar for both channels ($Br^- \approx Cl^- >$ acetate), the numeric value of the permeability ratio was notably different for acetate. The permeability ratio for glutamate$^-$ to Cl^- of 0.23 for the WT-MEF maxi-anion channels [14] was also different from the value of $P_{glutamate}/P_{Cl} = 0.4$ reported for the mitochondrial porin [175]. Although voltage-dependent gating has been considered to be a common property for the two channels, the mitochondrial VDAC is known to

Table 2 Comparison of the single-channel properties between the mitochondrial VDAC and the maxi-anion channel

Parameter	VDAC	Maxi-anion channel
P_{Cl}/P_K (100/1,000 mM KCl)	1.7–1.9 [173, 174]	13.5 ± 2.3 [14]
$P_{acetate}/P_{Cl}$	0.41 [178]	0.58 ± 0.01 [14]
$P_{glutamate}/P_{Cl}$	0.4 [175]	0.17 [108]; 0.23 [14]
$[Cl^-]$ dependence for single-channel conductance	Linear up to 10 nS with no saturation [173]	Saturates at 580–640 pS with Kd = 77–120 mM [24, 104, 113]
Pore size	1 and 2 nm for different entrances [179, 180]	1.16 and 1.42 nm for different entrances [11]
Voltage-dependent "closed" state	Retains ~40% of initial conductance [150]	Non-conductive [8, 14]

retain approximately 40% of its initial conductance in the so-called "closed" state, which is cation-selective [150, 151], whereas the maxi-anion channel closes completely at high positive and negative voltages (e.g. [8, 14]). Voltage-dependent modulation of ionic selectivity has never been reported for maxi-anion channels, supporting our conclusion that the maxi-anion channel and VDAC are unrelated proteins.

Plasmalemmal VDAC is not the only molecular candidate for the maxi-anion channel. Recently, Suzuki and Mizuno [176] have reported that a gene *tweety* found in *Drosophila flightless* locus has a structure similar to those of known channels. The human homologs of *tweety* (hTTYH1-3) have been suggested to provide a product, which represents a novel large-conductance Ca^{2+}-activated chloride channel, while a related gene hTTYH1 gave rise to functional expression of the swelling-activated chloride channel. It has been hypothesized that hTTYH1 might be the large-conductance Ca^{2+}-activated Cl^- channel [176, 177]. We attempted to check this attractive hypothesis by transfecting two splice-variant clones of the TTYH1 gene (TTYH1-E and TTYH1-SV, kind gifts from Dr. M. Suzuki) into HEK293T cells and assaying the maxi-anion channel activity 1–5 days after transfection by patch excision. In these experiments, either control, TTYH1-E- or TTYH1-SV-transfected cells never showed the maxi-anion channel phenotype typical to C127 cells used as a positive control in these experiments [13]. This result implies that the human homologs of *tweety* clones alone are unlikely to be molecular identity of the maxi-anion channel. We believe that more thorough tests of this attractive hypothesis are yet necessary. It might be meaningful to test some other variants of TTHY genes as well.

The maxi-anion channel in cardiomyocytes [2] and mammary C127 cells [137] was insensitive to octanol-1, suggesting that it is unrelated to connexins. A plasmalemmal subtype of the mitochondrial adenine nucleotide translocase (ANT), or ADP/ATP carrier (AAC), which mediates ATP/ADP exchange at the inner mitochondrial membrane, could also be ruled out based on the insensitivity of the maxi-anion channel to the potent and selective blockers of ANT, atractyloside and bongkrekic acid [137].

Taken together, we must summarize that the molecular entity of this classical channel has as yet been unidentified.

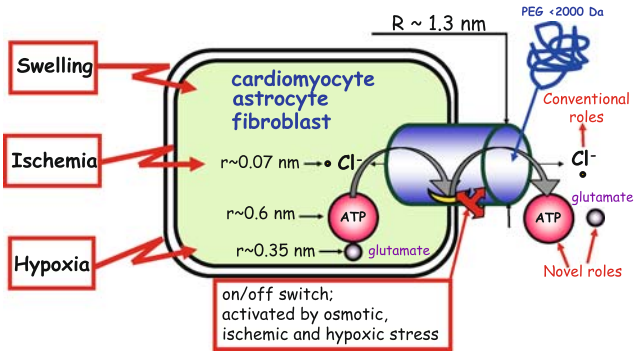

Fig. 10 Maxi-anion channel is activated by osmotic swelling, ischemia and hypoxia, and its pore serves as the conducting pathways not only for a small inorganic anion, Cl^-, but also for negatively charged signaling molecules, ATP and glutamate. Transport of Cl^- defines the conventional roles of the maxi-anion channel in fluid secretion/absorption, in cell volume regulation, and in controlling the membrane potential. On the other hand, the wide nano-sized pore of the maxi-anion channel is capable to release extracellular signals, ATP and glutamate, from a cell, thus defining novel roles of this channel in stress-sensory signal transduction. See text for details

Concluding remarks

The maxi-anion channel, which is activated by osmotic cell swelling, is ubiquitously expressed and found in almost every part of the body. This classical anion channel obviously fulfils important physiological functions, which remain incompletely understood at present. As a conventional chloride-conducting pathway, the maxi-anion channel is likely to be involved in controlling the cell membrane potential, in fluid secretion/absorption and in cell volume regulation (Fig. 10). However, the ability to

release small amounts of physiologically important signaling molecules, such as ATP and glutamate, puts this channel in the center of the purinergic and glutamatergic cell-to-cell signal transduction (Fig. 10). Also, this channel is deeply associated with the pathogenesis of cardiac ischemia and hypoxia as well as with excitotoxic neurodegeneration in the brain. With regard not only to its conventional roles due to Cl^- conduction but also to its novel roles due to signaling anion conduction (Fig. 10); therefore, the maxi-anion channel would represent an important target for drug discovery. The maxi-anion channel has recently been verified to possess a wide nanoscopic pore (Fig. 10). However, the channel molecule itself is not identified. Molecular identification of the maxi-anion channel is an urgent task that would greatly promote the studies in this field.

Acknowledgments We are grateful to T. Okayasu for manuscript preparation. This work was supported by Grant-in-Aid for Scientific Research (A) and those for Scientific Research on Priority Areas to YO and that for Scientific Research (C) to RZS from the Japan Society for the Promotion of Science and the Ministry of Education, Culture, Sports, Science and Technology of Japan, as well as Grants-in-Aid from the Center for Science and Technology and Academy of Sciences of Uzbekistan to RZS.

References

1. Okada Y (1997) Volume expansion-sensing outward-rectifier Cl^- channel: fresh start to the molecular identity and volume sensor. Am J Physiol 273:C755–C789
2. Dutta AK, Sabirov RZ, Uramoto H, Okada Y (2004) Role of ATP-conductive anion channel in ATP release from neonatal rat cardiomyocytes in ischaemic or hypoxic conditions. J Physiol 559:799–812
3. Falke LC, Misler S (1989) Activity of ion channels during volume regulation by clonal N1E115 neuroblastoma cells. Proc Natl Acad Sci USA 86:3919–3923. doi:10.1073/pnas.86.10.3919
4. Jalonen T (1993) Single-channel characteristics of the large-conductance anion channel in rat cortical astrocytes in primary culture. Glia 9:227–237. doi:10.1002/glia.440090308
5. Liu HT, Tashmukhamedov BA, Inoue H, Okada Y, Sabirov RZ (2006) Roles of two types of anion channels in glutamate release from mouse astrocytes under ischemic or osmotic stress. Glia 54:343–357. doi:10.1002/glia.20400
6. Liu HT, Sabirov RZ, Okada Y (2008) Oxygen-glucose deprivation induces ATP release via maxi-anion channels in astrocytes. Purinergic Signal 4:147–154. doi:10.1007/s11302-007-9077-8
7. Liu HT, Toychiev AH, Takahashi N, Sabirov RZ, Okada Y (2008) Maxi-anion channel as a candidate pathway for osmosensitive ATP release from mouse astrocytes in primary culture. Cell Res 18:558–565. doi:10.1038/cr.2008.49
8. Sabirov RZ, Dutta AK, Okada Y (2001) Volume-dependent ATP-conductive large-conductance anion channel as a pathway for swelling-induced ATP release. J Gen Physiol 118:251–266. doi:10.1085/jgp.118.3.251
9. Schwiebert EM, Mills JW, Stanton BA (1994) Actin-based cytoskeleton regulates a chloride channel and cell volume in a renal cortical collecting duct cell line. J Biol Chem 269:7081–7089
10. Sabirov RZ, Okada Y (2004) ATP-conducting maxi-anion channel: a new player in stress-sensory transduction. Jpn J Physiol 54:7–14. doi:10.2170/jjphysiol.54.7
11. Sabirov RZ, Okada Y (2004) Wide nanoscopic pore of maxi-anion channel suits its function as an ATP-conductive pathway. Biophys J 87:1672–1685. doi:10.1529/biophysj.104.043174
12. Dutta AK, Korchev YE, Shevchuk AI, Hayashi S, Okada Y, Sabirov RZ (2008) Spatial distribution of maxi-anion channel on cardiomyocytes detected by smart-patch technique. Biophys J 94:1646–1655. doi:10.1529/biophysj.107.117820
13. Okada Y, Sato K, Toychiev AH, Suzuki M, Dutta AK, Inoue H, Sabirov RZ (2009) The puzzles of volume-activated anion channels. In: Alvarez-Leefmans FJ, Delpire E (eds) Physiology and pathology of chloride transporters and channels in the nervous system from molecules to diseases. Elsevier, San Diego (in press)
14. Sabirov RZ, Sheiko T, Liu H, Deng D, Okada Y, Craigen WJ (2006) Genetic demonstration that the plasma membrane maxianion channel and voltage-dependent anion channels are unrelated proteins. J Biol Chem 281:1897–1904. doi:10.1074/jbc.M509482200
15. Strange K, Emma F, Jackson PS (1996) Cellular and molecular physiology of volume-sensitive anion channels. Am J Physiol Cell Physiol 270:C711–C730
16. Blatz AL, Magleby KL (1983) Single voltage-dependent chloride-selective channels of large conductance in cultured rat muscle. Biophys J 43:237–241
17. Schwarze W, Kolb HA (1984) Voltage-dependent kinetics of an anionic channel of large unit conductance in macrophages and myotube membranes. Pflugers Arch 402:281–291. doi:10.1007/BF00585511
18. Gray PT, Bevan S, Ritchie JM (1984) High conductance anion-selective channels in rat cultured Schwann cells. Proc R Soc Lond B Biol Sci 221:395–409
19. Nelson DJ, Tang JM, Palmer LG (1984) Single-channel recordings of apical membrane chloride conductance in A6 epithelial cells. J Membr Biol 80:81–89. doi:10.1007/BF01868692
20. Woll KH, Leibowitz MD, Neumcke B, Hille B (1987) A high-conductance anion channel in adult amphibian skeletal muscle. Pflugers Arch 410:632–640. doi:10.1007/BF00581324
21. Woll KH, Neumcke B (1987) Conductance properties and voltage dependence of an anion channel in amphibian skeletal muscle. Pflugers Arch 410:641–647. doi:10.1007/BF00581325
22. Dixon DM, Valkanov M, Martin RJ (1993) A patch-clamp study of the ionic selectivity of the large conductance, Ca-activated chloride channel in muscle vesicles prepared from *Ascaris suum*. J Membr Biol 131:143–149. doi:10.1007/BF02791323
23. Hurnak O, Zachar J (1992) Maxi chloride channels in L6 myoblasts. Gen Physiol Biophys 11:389–400
24. Hurnak O, Zachar J (1994) Conductance–voltage relations in large-conductance chloride channels in proliferating L6 myoblasts. Gen Physiol Biophys 13:171–192
25. Hurnak O, Zachar J (1995) Selectivity of maxi chloride channels in the L6 rat muscle cell line. Gen Physiol Biophys 14:91–105
26. Zachar J, Hurnak O (1994) Arachidonic acid blocks large-conductance chloride channels in L6 myoblasts. Gen Physiol Biophys 13:193–213
27. Hurnak O, Zachar J (1993) High-conductance chloride channels in BC3H1 myoblasts. Gen Physiol Biophys 12:171–182
28. Coleman HA, Parkington HC (1987) Single channel Cl^- and K^+ currents from cells of uterus not treated with enzymes. Pflugers Arch 410:560–562. doi:10.1007/BF00586540
29. Sun XP, Supplisson S, Mayer E (1993) Chloride channels in myocytes from rabbit colon are regulated by a pertussis toxin-sensitive G protein. Am J Physiol 264:G774–G785

30. Sun XP, Supplisson S, Torres R, Sachs G, Mayer E (1992) Characterization of large-conductance chloride channels in rabbit colonic smooth muscle. J Physiol 448:355–382
31. Kokubun S, Saigusa A, Tamura T (1991) Blockade of Cl channels by organic and inorganic blockers in vascular smooth muscle cells. Pflugers Arch 418:204–213. doi:10.1007/BF00370515
32. Saigusa A, Kokubun S (1988) Protein kinase C may regulate resting anion conductance in vascular smooth muscle cells. Biochem Biophys Res Commun 155:882–889. doi:10.1016/S0006-291X(88)80578-3
33. Soejima M, Kokubun S (1988) Single anion-selective channel and its ion selectivity in the vascular smooth muscle cell. Pflugers Arch 411:304–311. doi:10.1007/BF00585119
34. Coulombe A, Coraboeuf E (1992) Large-conductance chloride channels of new-born rat cardiac myocytes are activated by hypotonic media. Pflugers Arch 422:143–150. doi:10.1007/BF00370413
35. Coulombe A, Duclohier H, Coraboeuf E, Touzet N (1987) Single chloride-permeable channels of large conductance in cultured cardiac cells of new-born rats. Eur Biophys J 14:155–162. doi:10.1007/BF00253840
36. Hussy N (1992) Calcium-activated chloride channels in cultured embryonic *Xenopus* spinal neurons. J Neurophysiol 68:2042–2050
37. Wu JV, Shrager P (1994) Resolving three types of chloride channels in demyelinated *Xenopus* axons. J Neurosci Res 38:613–620. doi:10.1002/jnr.490380603
38. Bahamonde MI, Fernandez-Fernandez JM, Guix FX, Vazquez E, Valverde MA (2003) Plasma membrane voltage-dependent anion channel mediates antiestrogen-activated maxi Cl^- currents in C1300 neuroblastoma cells. J Biol Chem 278:33284–33289. doi:10.1074/jbc.M302814200
39. Bettendorff L (1996) A non-cofactor role of thiamine derivatives in excitable cells? Arch Physiol Biochem 104:745–751. doi:10.1076/apab.104.6.745.12916
40. Bettendorff L, Kolb HA, Schoffeniels E (1993) Thiamine triphosphate activates an anion channel of large unit conductance in neuroblastoma cells. J Membr Biol 136:281–288. doi:10.1007/BF00233667
41. Bolotina V, Borecky J, Vlachovà V, Baudysova M, Vyskocil F (1987) Voltage-dependent chloride channels with several substates in excised patches from mouse neuroblastoma cells. Neurosci Lett 77:298–302. doi:10.1016/0304-3940(87)90516-7
42. Diaz M, Bahamonde MI, Lock H, Munoz FJ, Hardy SP, Posas F, Valverde MA (2001) Okadaic acid-sensitive activation of Maxi Cl^- channels by triphenylethylene antioestrogens in C1300 mouse neuroblastoma cells. J Physiol 536:79–88. doi:10.1111/j.1469-7793.2001.00079.x
43. Forshaw PJ, Lister T, Ray DE (1993) Inhibition of a neuronal voltage-dependent chloride channel by the type II pyrethroid, deltamethrin. Neuropharmacology 32:105–111. doi:10.1016/0028-3908(93)90089-L
44. Forshaw PJ, Lister T, Ray DE (2000) The role of voltage-gated chloride channels in type II pyrethroid insecticide poisoning. Toxicol Appl Pharmacol 163:1–8. doi:10.1006/taap.1999.8848
45. Akanda N, Elinder F (2006) Biophysical properties of the apoptosis-inducing plasma membrane voltage-dependent anion channel. Biophys J 90:4405–4417. doi:10.1529/biophysj.105.080028
46. Elinder F, Akanda N, Tofighi R, Shimizu S, Tsujimoto Y, Orrenius S, Ceccatelli S (2005) Opening of plasma membrane voltage-dependent anion channels (VDAC) precedes caspase activation in neuronal apoptosis induced by toxic stimuli. Cell Death Differ 12(8):1134–1140
47. McLarnon JG, Kim SU (1991) Ion channels in cultured adult human Schwann cells. Glia 4:534–539. doi:10.1002/glia.440040513
48. Quasthoff S, Strupp M, Grafe P (1992) High conductance anion channel in Schwann cell vesicles from rat spinal roots. Glia 5:17–24. doi:10.1002/glia.440050104
49. Dermietzel R, Hwang TK, Buettner R, Hofer A, Dotzler E, Kremer M, Deutzmann R, Thinnes FP, Fishman GI, Spray DC (1994) Cloning and in situ localization of a brain-derived porin that constitutes a large-conductance anion channel in astrocytic plasma membranes. Proc Natl Acad Sci USA 91:499–503. doi:10.1073/pnas.91.2.499
50. Sonnhof U (1987) Single voltage-dependent K^+ and Cl^- channels in cultured rat astrocytes. Can J Physiol Pharmacol 65:1043–1050
51. Nowak L, Ascher P, Berwald-Netter Y (1987) Ionic channels in mouse astrocytes in culture. J Neurosci 7:101–109
52. Guibert B, Dermietzel R, Siemen D (1998) Large conductance channel in plasma membranes of astrocytic cells is functionally related to mitochondrial VDAC-channels. Int J Biochem Cell Biol 30:379–391. doi:10.1016/S1357-2725(97)00137-4
53. Hanrahan JW, Alles WP, Lewis SA (1985) Single anion-selective channels in basolateral membrane of a mammalian tight epithelium. Proc Natl Acad Sci USA 82:7791–7795. doi:10.1073/pnas.82.22.7791
54. Kajita H, Kotera T, Shirakata Y, Ueda S, Okuma M, Oda-Ohmae K, Takimoto M, Urade Y, Okada Y (1995) A maxi Cl^- channel coupled to endothelin B receptors in the basolateral membrane of guinea-pig parietal cells. J Physiol 488:65–75
55. Becq F, Fanjul M, Mahieu I, Berger Z, Gola M, Hollande E (1992) Anion channels in a human pancreatic cancer cell line (Capan-1) of ductal origin. Pflugers Arch 420:46–53. doi:10.1007/BF00378640
56. Duszyk M, Liu D, French AS, Man SF (1993) Halide permeation through three types of epithelial anion channels after reconstitution into giant liposomes. Eur Biophys J 22:5–11. doi:10.1007/BF00205807
57. Duszyk M, Liu D, French AS, Man SF (1995) Evidence that pH-titratable groups control the activity of a large epithelial chloride channel. Biochem Biophys Res Commun 215:355–360. doi:10.1006/bbrc.1995.2473
58. Bajnath RB, Groot JA, de Jonge HR, Kansen M, Bijman J (1993) Calcium ionophore plus excision induce a large conductance chloride channel in membrane patches of human colon carcinoma cells HT-29cl.19A. Experientia 49:313–316. doi:10.1007/BF01923409
59. Morris AP, Frizzell RA (1993) Ca^{2+}-dependent Cl^- channels in undifferentiated human colonic cells (HT-29). II. Regulation and rundown. Am J Physiol 264:C977–C985
60. Vaca L, Kunze DL (1992) Anion and cation permeability of a large conductance anion channel in the T84 human colonic cell line. J Membr Biol 130:241–249. doi:10.1007/BF00240481
61. Kemp PJ, MacGregor GG, Olver RE (1993) G protein-regulated large-conductance chloride channels in freshly isolated fetal type II alveolar epithelial cells. Am J Physiol 265:L323–L329
62. Krouse ME, Schneider GT, Gage PW (1986) A large anion-selective channel has seven conductance levels. Nature 319:58–60. doi:10.1038/319058a0
63. Schneider GT, Cook DI, Gage PW, Young JA (1985) Voltage sensitive, high-conductance chloride channels in the luminal membrane of cultured pulmonary alveolar (type II) cells. Pflugers Arch 404:354–357. doi:10.1007/BF00585348
64. Garner C, Brown PD (1992) Two types of chloride channel in the apical membrane of rat choroid plexus epithelial cells. Brain Res 591:137–145. doi:10.1016/0006-8993(92)90988-L
65. McGill JM, Basavappa S, Fitz JG (1992) Characterization of high-conductance anion channels in rat bile duct epithelial cells. Am J Physiol 262:G703–G710

66. McGill JM, Gettys TW, Basavappa S, Fitz JG (1993) GTP-binding proteins regulate high conductance anion channels in rat bile duct epithelial cells. J Membr Biol 133:253–261. doi:10.1007/BF00232024
67. Do CW, Peterson-Yantorno K, Mitchell CH, Civan MM (2004) cAMP-activated maxi-Cl^- channels in native bovine pigmented ciliary epithelial cells. Am J Physiol Cell Physiol 287:C1003–C1011. doi:10.1152/ajpcell.00175.2004
68. Mitchell CH, Wang L, Jacob TJC (1997) A large-conductance chloride channel in pigmented ciliary epithelial cells activated by GTPgammaS. J Membr Biol 158:167–175. doi:10.1007/s002329900254
69. Zhang JJ, Jacob TJ (1997) Three different Cl^- channels in the bovine ciliary epithelium activated by hypotonic stress. J Physiol 499:379–389
70. Bell PD, Lapointe JY, Sabirov R, Hayashi S, Peti-Peterdi J, Manabe K, Kovacs G, Okada Y (2003) Macula densa cell signaling involves ATP release through a maxi anion channel. Proc Natl Acad Sci USA 100:4322–4327. doi:10.1073/pnas.0736323100
71. Dietl P, Stanton BA (1992) Chloride channels in apical and basolateral membranes of CCD cells (RCCT-28A) in culture. Am J Physiol 263:F243–F250
72. Kolb HA, Brown CD, Murer H (1985) Identification of a voltage-dependent anion channel in the apical membrane of a Cl^--secretory epithelium (MDCK). Pflugers Arch 403:262–265. doi:10.1007/BF00583597
73. Light DB, Schwiebert EM, Fejes-Toth G, Naray-Fejes-Toth A, Karlson KH, McCann FV, Stanton BA (1990) Chloride channels in the apical membrane of cortical collecting duct cells. Am J Physiol 258:F273–F280
74. O'Donnell MJ, Rheault MR, Davies SA, Rosay P, Harvey BJ, Maddrell SH, Kaiser K, Dow JA (1998) Hormonally controlled chloride movement across *Drosophila* tubules is via ion channels in stellate cells. Am J Physiol 274:R1039–R1049
75. Schwiebert EM, Karlson KH, Friedman PA, Dietl P, Spielman WS, Stanton BA (1992) Adenosine regulates a chloride channel via protein kinase C and a G protein in a rabbit cortical collecting duct cell line. J Clin Invest 89:834–841. doi:10.1172/JCI115662
76. Schwiebert EM, Light DB, Fejes-Toth G, Naray-Fejes-Toth A, Stanton BA (1990) A GTP-binding protein activates chloride channels in a renal epithelium. J Biol Chem 265:7725–7728
77. Velasco G, Prieto M, Alvarez-Riera J, Gascon S, Barros F (1989) Characteristics and regulation of a high conductance anion channel in GBK kidney epithelial cells. Pflugers Arch 414:304–310. doi:10.1007/BF00584631
78. Zhu G, Zhang Y, Xu H, Jiang C (1998) Identification of endogenous outward currents in the human embryonic kidney (HEK 293) cell line. J Neurosci Methods 81:73–83. doi:10.1016/S0165-0270(98)00019-3
79. Marcus DC, Takeuchi S, Wangemann P (1993) Two types of chloride channel in the basolateral membrane of vestibular dark cells. Hear Res 69:124–132. doi:10.1016/0378-5955(93)90100-F
80. Bernucci L, Umana F, Llanos P, Riquelme G (2003) Large chloride channel from pre-eclamptic human placenta. Placenta 24:895–903. doi:10.1016/S0143-4004(03)00144-9
81. Brown PD, Greenwood SL, Robinson J, Boyd RD (1993) Chloride channels of high conductance in the microvillous membrane of term human placenta. Placenta 14:103–115. doi:10.1016/S0143-4004(05)80253-X
82. Henriquez M, Riquelme G (2003) 17b-estradiol and tamoxifen regulate a maxi-chloride channel from human placenta. J Membr Biol 191:59–68. doi:10.1007/s00232-002-1038-0
83. Riquelme G, Llanos P, Tischner E, Neil J, Campos B (2004) Annexin 6 modulates the maxi-chloride channel of the apical membrane of syncytiotrophoblast isolated from human placenta. J Biol Chem 279:50601–50608. doi:10.1074/jbc.M407859200
84. Riquelme G, Parra M (1999) Regulation of human placental chloride channel by arachidonic acid and other cis unsaturated fatty acids. Am J Obstet Gynecol 180:469–475. doi:10.1016/S0002-9378(99)70234-6
85. Riquelme G, Stutzin A, Barros LF, Liberona JL (1995) A chloride channel from human placenta reconstituted into giant liposomes. Am J Obstet Gynecol 173:733–738. doi:10.1016/0002-9378(95)90332-1
86. Riquelme G (2006) Apical Maxi-chloride channel from human placenta: 12 years after the first electrophysiological recordings. Biol Res 39:437–445
87. Stumpff F, Martens H, Bilk S, Aschenbach JR, Gabel G (2008) Cultured ruminal epithelial cells express a large-conductance channel permeable to chloride, bicarbonate, and acetate. Pflugers Arch. doi:10.1007/s00424-008-0566-6
88. Bahamonde MI, Valverde MA (2003) Voltage-dependent anion channel localises to the plasma membrane and peripheral but not perinuclear mitochondria. Pflugers Arch 446:309–313
89. Hardy SP, Valverde MA (1994) Novel plasma membrane action of estrogen and antiestrogens revealed by their regulation of a large conductance chloride channel. FASEB J 8:760–765
90. Kawahara K, Takuwa N (1991) Bombesin activates large-conductance chloride channels in Swiss 3T3 fibroblasts. Biochem Biophys Res Commun 177:292–298. doi:10.1016/0006-291X(91)91981-H
91. Nobile M, Galietta LJ (1988) A large conductance Cl^- channel revealed by patch-recordings in human fibroblasts. Biochem Biophys Res Commun 154:719–726. doi:10.1016/0006-291X(88)90199-4
92. Mangel AW, Raymond JR, Fitz JG (1993) Regulation of high-conductance anion channels by G proteins and 5-HT1A receptors in CHO cells. Am J Physiol Renal Physiol 264:F490–F495
93. Groschner K, Kukovetz WR (1992) Voltage-sensitive chloride channels of large conductance in the membrane of pig aortic endothelial cells. Pflugers Arch 421:209–217. doi:10.1007/BF00374829
94. Li Z, Niwa Y, Sakamoto S, Chen X, Nakaya Y (2000) Estrogen modulates a large conductance chloride channel in cultured porcine aortic endothelial cells. J Cardiovasc Pharmacol 35:506–510. doi:10.1097/00005344-200003000-00023
95. Olesen SP, Bundgaard M (1992) Chloride-selective channels of large conductance in bovine aortic endothelial cells. Acta Physiol Scand 144:191–198
96. Vaca L (1999) SITS blockade induces multiple subconductance states in a large conductance chloride channel. J Membr Biol 169:65–73. doi:10.1007/PL00005902
97. Vaca L, Kunze DL (1993) cAMP-dependent phosphorylation modulates voltage gating in an endothelial Cl^- channel. Am J Physiol 264:C370–C375
98. Bosma MM (1989) Anion channels with multiple conductance levels in a mouse B lymphocyte cell line. J Physiol 410:67–90
99. McCann FV, McCarthy DC, Keller TM, Noelle RJ (1989) Characterization of a large conductance non-selective anion channel in B lymphocytes. Cell Signal 1:31–44. doi:10.1016/0898-6568(89)90018-1
100. McCann FV, McCarthy DC, Noelle RJ (1990) Patch-clamp profile of ion channels in resting murine B lymphocytes. J Membr Biol 114:175–188. doi:10.1007/BF01869098
101. Yeh TH, Tsai MC, Lee SY, Hsu MM (1996) Characterization and relative abundance of maxi-chloride channels in Epstein-Barr virus (EBV) producer: B95-8 cells. Experientia 52:818–826. doi:10.1007/BF01923996
102. Cahalan MD, Lewis RS (1988) Role of potassium and chloride channels in volume regulation by T lymphocytes. In: Gunn RB,

Parker JC (eds) Cell physiology of blood. Rockefeller University Press, New York, pp 281–301
103. Pahapill PA, Schlichter LC (1992) Cl^- channels in intact human T lymphocytes. J Membr Biol 125:171–183. doi:10.1007/BF00233356
104. Schlichter LC, Grygorczyk R, Pahapill PA, Grygorczyk C (1990) A large, multiple-conductance chloride channel in normal human T lymphocytes. Pflugers Arch 416:413–421. doi:10.1007/BF00370748
105. Kolb HA, Ubl J (1987) Activation of anion channels by zymosan particles in membranes of peritoneal macrophages. Biochim Biophys Acta 899:239–246. doi:10.1016/0005-2736(87)90405-6
106. Lindau M, Fernandez JM (1986) A patch-clamp study of histamine-secreting cells. J Gen Physiol 88:349–368. doi:10.1085/jgp.88.3.349
107. Wohlrab D, Wohlrab J, Markwardt F (2000) Electrophysiological characterization of human keratinocytes using the patch-clamp technique. Exp Dermatol 9:219–223. doi:10.1034/0625.2000.009003219.x
108. Ravesloot JH, Van Houten RJ, Ypey DL, Nijweide PJ (1991) High-conductance anion channels in embryonic chick osteogenic cells. J Bone Miner Res 6:355–363
109. Stea A, Nurse CA (1989) Chloride channels in cultured glomus cells of the rat carotid body. Am J Physiol 257:C174–C181
110. Buettner R, Papoutsoglou G, Scemes E, Spray DC, Dermietzel R (2000) Evidence for secretory pathway localization of a voltage-dependent anion channel isoform. Proc Natl Acad Sci USA 97:3201–3206. doi:10.1073/pnas.060242297
111. O'Donnell MJ, Kelly SP, Nurse CA, Wood CM (2001) A maxi Cl^- channel in cultured pavement cells from the gills of the freshwater rainbow trout *Oncorhynchus mykiss*. J Exp Biol 204:1783–1794
112. Dutta AK, Okada Y, Sabirov RZ (2002) Regulation of an ATP-conductive large-conductance anion channel and swelling-induced ATP release by arachidonic acid. J Physiol 542:803–816. doi:10.1113/jphysiol.2002.019802
113. Hals GD, Stein PG, Palade PT (1989) Single channel characteristics of a high conductance anion channel in "sarcoballs". J Gen Physiol 93:385–410. doi:10.1085/jgp.93.3.385
114. Schmid A, Gogelein H, Kemmer TP, Schulz I (1988) Anion channels in giant liposomes made of endoplasmic reticulum vesicles from rat exocrine pancreas. J Membr Biol 104:275–282. doi:10.1007/BF01872329
115. Thompson RJ, Nordeen MH, Howell KE, Caldwell JH (2002) A large-conductance anion channel of the Golgi complex. Biophys J 83:278–289
116. Klenerman D, Korchev Y (2006) Potential biomedical applications of the scanned nanopipette. Nanomed 1:107–114. doi:10.2217/17435889.1.1.107
117. Korchev YE, Bashford CL, Milovanovic M, Vodyanoy I, Lab MJ (1997) Scanning ion conductance microscopy of living cells. Biophys J 73:653–658
118. Korchev YE, Negulyaev YA, Edwards CR, Vodyanoy I, Lab MJ (2000) Functional localization of single active ion channels on the surface of a living cell. Nat Cell Biol 2:616–619. doi:10.1038/35023563
119. Ternovsky VI, Okada Y, Sabirov RZ (2004) Sizing the pore of the volume-sensitive anion channel by differential polymer partitioning. FEBS Lett 576:433–436. doi:10.1016/j.febslet.2004.09.051
120. Krasilnikov OV, Sabirov RZ, Okada Y (2007) Probing pore geometry of the CFTR channel by polymer partitioning. XXXII Brazilian Biophysical Society Meeting, Abstract. Aguas de Lindoia, Brazil
121. Fan H-T, Morishima S, Kida H, Okada Y (2001) Phloretin differentially inhibits volume-sensitive and cyclic AMP-activated, but not Ca-activated, Cl^- channels. Br J Pharmacol 133:1096–1106. doi:10.1038/sj.bjp.0704159
122. Liu Y, Oiki S, Tsumura T, Shimizu T, Okada Y (1998) Glibenclamide blocks volume-sensitive Cl^- channels by dual mechanisms. Am J Physiol Cell Physiol 275:C343–C351
123. Boudreault F, Grygorczyk R (2002) Cell swelling-induced ATP release and gadolinium-sensitive channels. Am J Physiol Cell Physiol 282:C219–C226
124. Roman RM, Feranchak AP, Davison AK, Schwiebert EM, Fitz JG (1999) Evidence for Gd^{3+} inhibition of membrane ATP permeability and purinergic signaling. Am J Physiol 277:G1222–G1230
125. Hazama A, Shimizu T, Ando-Akatsuka Y, Hayashi S, Tanaka S, Maeno E, Okada Y (1999) Swelling-induced, CFTR-independent ATP release from a human epithelial cell line: lack of correlation with volume-sensitive Cl^- channels. J Gen Physiol 114:525–533. doi:10.1085/jgp.114.4.525
126. Lang F, Busch GL, Ritter M, Volkl H, Waldegger S, Gulbins E, Haussinger D (1998) Functional significance of cell volume regulatory mechanisms. Physiol Rev 78:247–306
127. Wehner F, Olsen H, Tinel H, Kinne-Saffran E, Kinne RK (2003) Cell volume regulation: osmolytes, osmolyte transport, and signal transduction. Rev Physiol Biochem Pharmacol 148:1–80. doi:10.1007/s10254-003-0009-x
128. Mills JW, Schwiebert EM, Stanton BA (1994) The cytoskeleton and membrane transport. Curr Opin Nephrol Hypertens 3:529–534. doi:10.1097/00041552-199409000-00009
129. Vallejos C, Riquelme G (2007) The maxi-chloride channel in human syncytiotrophoblast: a pathway for taurine efflux in placental volume regulation? Placenta 28:1182–1191. doi:10.1016/j.placenta.2007.06.005
130. Do CW, Civan MM (2006) Swelling-activated chloride channels in aqueous humour formation: on the one side and the other. Acta Physiol 187:345–352. doi:10.1111/j.1748-1716.2006.01548.x
131. Bodin P, Burnstock G (2001) Purinergic signalling: ATP release. Neurochem Res 26:959–969. doi:10.1023/A:1012388618693
132. Dubyak GR, el Moatassim C (1993) Signal transduction via P2-purinergic receptors for extracellular ATP and other nucleotides. Am J Physiol 265:C577–C606
133. Fields RD, Stevens B (2000) ATP: an extracellular signaling molecule between neurons and glia. Trends Neurosci 23:625–633. doi:10.1016/S0166-2236(00)01674-X
134. Forrester T (2003) A purine signal for functional hypertemia in skeletal and cardiac muscle. In: Schwiebert EM (ed) Current topics in membranes: extracellular nucleotides and nucleosides: release, receptors, and physiological & pathophysiological effects (current topics in membranes, vol 54). Academic Press, Amsterdam, pp 269–305
135. Ralevic V, Burnstock G (1998) Receptors for purines and pyrimidines. Pharmacol Rev 50:413–492
136. Burnstock G (2004) Introduction: P2 receptors. Curr Top Med Chem 4:793–803. doi:10.2174/1568026043451014
137. Sabirov RZ, Okada Y (2005) ATP release via anion channels. Purinergic Signal 1:311–328. doi:10.1007/s11302-005-1557-0
138. Gu Y, Gorelik J, Spohr HA, Shevchuk A, Lab MJ, Harding SE, Vodyanoy I, Klenerman D, Korchev YE (2002) High-resolution scanning patch-clamp: new insights into cell function. FASEB J 16:748–750
139. Hazama A, Hayashi S, Okada Y (1998) Cell surface measurements of ATP release from single pancreatic beta cells using a novel biosensor technique. Pflugers Arch 437:31–35. doi:10.1007/s004240050742

140. Hayashi S, Hazama A, Dutta AK, Sabirov RZ, Okada Y (2004) Detecting ATP release by a biosensor method. Sci STKE 2004:pl14
141. Bell PD, Lapointe JY, Peti-Peterdi J (2003) Macula densa cell signaling. Annu Rev Physiol 65:481–500. doi:10.1146/annurev.physiol.65.050102.085730
142. Uchida S, Sasaki S (2005) Function of chloride channels in the kidney. Annu Rev Physiol 67:759–778. doi:10.1146/annurev.physiol.67.032003.153547
143. Haydon PG (2001) GLIA: listening and talking to the synapse. Nat Rev Neurosci 2:185–193. doi:10.1038/35058528
144. Hansson E, Ronnback L (2003) Glial neuronal signaling in the central nervous system. FASEB J 17:341–348. doi:10.1096/fj.02-0429rev
145. Nedergaard M, Takano T, Hansen AJ (2002) Beyond the role of glutamate as a neurotransmitter. Nat Rev Neurosci 3:748–755. doi:10.1038/nrn916
146. Phillis JW, O'Regan MH (2003) Characterization of modes of release of amino acids in the ischemic/reperfused rat cerebral cortex. Neurochem Int 43:461–467. doi:10.1016/S0197-0186(03)00035-4
147. Kimelberg HK (2000) Cell volume in the CNS: regulation and implications for nervous system function and pathology. Neuroscientist 6:14–25. doi:10.1177/107385840000600110
148. Kimelberg HK (2004) Water homeostasis in the brain: basic concepts. Neuroscience 129:851–860. doi:10.1016/j.neuroscience.2004.07.033
149. Kimelberg HK, Nestor NB, Feustel PJ (2004) Inhibition of release of taurine and excitatory amino acids in ischemia and neuroprotection. Neurochem Res 29:267–274. doi:10.1023/B:NERE.0000010455.78121.53
150. Colombini M (2004) VDAC: the channel at the interface between mitochondria and the cytosol. Mol Cell Biochem 256–257:107–115. doi:10.1023/B:MCBI.0000009862.17396.8d
151. Colombini M, Blachly-Dyson E, Forte M (1996) VDAC, a channel in the outer mitochondrial membrane. In: Narahashi T (ed) Ion channels. Plenum Press, New York, pp 169–202
152. Mannella CA (1997) Minireview: on the structure and gating mechanism of the mitochondrial channel, VDAC. J Bioenerg Biomembr 29:525–531. doi:10.1023/A:1022489832594
153. Bathori G, Parolini I, Tombola F, Szabo I, Messina A, Oliva M, De Pinto V, Lisanti M, Sargiacomo M, Zoratti M (1999) Porin is present in the plasma membrane where it is concentrated in caveolae and caveolae-related domains. J Biol Chem 274:29607–29612. doi:10.1074/jbc.274.42.29607
154. Eben-Brunnen J, Reymann S, Awni LA, Cole T, Hellmann T, Hellmann KP, Paetzold G, Kleineke J, Thinnes FP, Gotz H, Hilschmann N (1998) Lentil lectin enriched microsomes from the plasma membrane of the human B-lymphocyte cell line H2LCL carry a heavy load of type-1 porin. Biol Chem 379:1419–1426
155. Jakob C, Gotz H, Hellmann T, Hellmann KP, Reymann S, Florke H, Thinnes FP, Hilschmann N (1995) Studies on human porin: XIII. The type-1 VDAC 'porin 31HL' biotinylated at the plasmalemma of trypan blue excluding human B lymphocytes. FEBS Lett 368:5–9. doi:10.1016/0014-5793(95)00465-L
156. Moon JI, Jung YW, Ko BH, De Pinto V, Jin I, Moon IS (1999) Presence of a voltage-dependent anion channel 1 in the rat postsynaptic density fraction. NeuroReport 10:443–447. doi:10.1097/00001756-199902250-00001
157. Puchelle E, Jacquot J, Fuchey C, Burlet H, Klossek JM, Gilain L, Triglia JM, Thinnes FP, Hilschmann N (1993) Studies on human porin. IX. Immunolocalization of porin and CFTR channels in human surface respiratory epithelium. Biol Chem Hoppe Seyler 374:297–304
158. Schwarzer C, Becker S, Awni LA, Cole T, Merker R, Barnikol-Watanabe S, Thinnes FP, Hilschmann N (2000) Human voltage-dependent anion-selective channel expressed in the plasmalemma of *Xenopus laevis* oocytes. Int J Biochem Cell Biol 32:1075–1084. doi:10.1016/S1357-2725(00)00047-9
159. Shimizu S, Matsuoka Y, Shinohara Y, Yoneda Y, Tsujimoto Y (2001) Essential role of voltage-dependent anion channel in various forms of apoptosis in mammalian cells. J Cell Biol 152:237–250. doi:10.1083/jcb.152.2.237
160. Steinacker P, Awni LA, Becker S, Cole T, Reymann S, Hesse D, Kratzin HD, Morris-Wortmann C, Schwarzer C, Thinnes FP, Hilschmann N (2000) The plasma membrane of *Xenopus laevis* oocytes contains voltage-dependent anion-selective porin channels. Int J Biochem Cell Biol 32:225–234. doi:10.1016/S1357-2725(99)00124-7
161. Thinnes FP, Gotz H, Kayser H, Benz R, Schmidt WE, Kratzin HD, Hilschmann N (1989) Identification of human porins. I. Purification of a porin from human B-lymphocytes (Porin 31HL) and the topochemical proof of its expression on the plasmalemma of the progenitor cell. Biol Chem Hoppe Seyler 370:1253–1264
162. Bathori G, Parolini I, Szabo I, Tombola F, Messina A, Oliva M, Sargiacomo M, De Pinto V, Zoratti M (2000) Extramitochondrial porin: facts and hypotheses. J Bioenerg Biomembr 32:79–89. doi:10.1023/A:1005516513313
163. Anflous K, Armstrong DD, Craigen WJ (2001) Altered mitochondrial sensitivity for ADP and maintenance of creatine-stimulated respiration in oxidative striated muscles from VDAC1-deficient mice. J Biol Chem 276:1954–1960. doi:10.1074/jbc.M006587200
164. Blachly-Dyson E, Zambronicz EB, Yu WH, Adams V, McCabe ER, Adelman J, Colombini M, Forte M (1993) Cloning and functional expression in yeast of two human isoforms of the outer mitochondrial membrane channel, the voltage-dependent anion channel. J Biol Chem 268:1835–1841
165. Bureau MH, Khrestchatisky M, Heeren MA, Zambrowicz EB, Kim H, Grisar TM, Colombini M, Tobin AJ, Olsen RW (1992) Isolation and cloning of a voltage-dependent anion channel-like Mr 36,000 polypeptide from mammalian brain. J Biol Chem 267:8679–8684
166. Ha H, Hajek P, Bedwell DM, Burrows PD (1993) A mitochondrial porin cDNA predicts the existence of multiple human porins. J Biol Chem 268:12143–12149
167. Rahmani Z, Maunoury C, Siddiqui A (1998) Isolation of a novel human voltage-dependent anion channel gene. Eur J Hum Genet 6:337–340. doi:10.1038/sj.ejhg.5200198
168. Sampson MJ, Lovell RS, Craigen WJ (1996) Isolation, characterization, and mapping of two mouse mitochondrial voltage-dependent anion channel isoforms. Genomics 33:283–288. doi:10.1006/geno.1996.0193
169. Sampson MJ, Lovell RS, Davison DB, Craigen WJ (1996) A novel mouse mitochondrial voltage-dependent anion channel gene localizes to chromosome 8. Genomics 36:192–196. doi:10.1006/geno.1996.0445
170. Sampson MJ, Ross L, Decker WK, Craigen WJ (1998) A novel isoform of the mitochondrial outer membrane protein VDAC3 via alternative splicing of a 3-base exon. Functional characteristics and subcellular localization. J Biol Chem 273:30482–30486. doi:10.1074/jbc.273.46.30482
171. Gonzalez-Gronow M, Kalfa T, Johnson CE, Gawdi G, Pizzo SV (2003) The voltage-dependent anion channel is a receptor for plasminogen kringle 5 on human endothelial cells. J Biol Chem 278:27312–27318. doi:10.1074/jbc.M303172200
172. Baker MA, Lane DJ, Ly JD, De Pinto V, Lawen A (2004) VDAC1 is a transplasma membrane NADH-ferricyanide

reductase. J Biol Chem 279:4811–4819. doi:10.1074/jbc.M311020200
173. Colombini M (1986) Voltage gating in VDAC: toward a molecular mechanism. In: Miller C (ed) Ion channel reconstitution. Plenum Press, New York, pp 533–550
174. Blachly-Dyson E, Peng S, Colombini M, Forte M (1990) Selectivity changes in site-directed mutants of the VDAC ion channel: structural implications. Science 247:1233–1236. doi:10.1126/science.1690454
175. Gincel D, Silberberg SD, Shoshan-Barmatz V (2000) Modulation of the voltage-dependent anion channel (VDAC) by glutamate. J Bioenerg Biomembr 32:571–583. doi:10.1023/A:1005670527340
176. Suzuki M, Mizuno A (2004) A novel human Cl^- channel family related to *Drosophila* flightless locus. J Biol Chem 279:22461–22468. doi:10.1074/jbc.M313813200
177. Suzuki M (2006) The *Drosophila* tweety family: molecular candidates for large-conductance Ca^{2+}-activated Cl^- channels. Exp Physiol 91:141–147. doi:10.1113/expphysiol.2005.031773
178. Zizi M, Byrd C, Boxus R, Colombini M (1998) The voltage-gating process of the voltage-dependent anion channel is sensitive to ion flow. Biophys J 75:704–713
179. Carneiro CMM, Krasilnikov OV, Yuldasheva LN, Campos de Carvalho AC, Nogueira RA (1997) Is the mammalian porin channel, VDAC, a perfect cylinder in the high conductance state? FEBS Lett 416:187–189. doi:10.1016/S0014-5793(97)01198-8
180. Carneiro CMM, Merzlyak PG, Yuldasheva LN, Silva LG, Thinnes FP, Krasilnikov OV (2003) Probing the volume changes during voltage gating of Porin 31BM channel with nonelectrolyte polymers. Biochim Biophys Acta 1612:144–153. doi:10.1016/S0005-2736(03)00113-5